A Systems Engineering V-Model Approach to the Tolerance Based Redesign of a Military Terrain Vehicle Suspension

by

Ivo van den Enden

Student number:	5376378
Thesis supervisor:	J. Herder
Company supervisor:	J. Cobben
Project Duration:	February 2025 - October 2025
Faculty:	Mechanical Engineering, Delft University of Technology

TU Delft

Preface

This thesis was written in partial fulfillment of the requirements for the MSc degree in Mechanical Engineering at Delft University of Technology. The work was carried out during an internship at a company specializing in the development of military terrain vehicles. The project follows the redesign of a military terrain vehicle suspension following the Systems Engineering V-Model approach.

I would like to thank Just Herder, my supervisor at the university, as well as my supervisor and colleagues at the company, for their valuable guidance and support during this project.

This report consists of two parts: a literature review and a redesign study. The literature review provides an overview of suspension systems for military terrain vehicles, outlining performance criteria and design considerations. Building on this overview, the redesign study applies the Systems Engineering V-Model approach to the redesign of the suspension system for a military terrain vehicle.
Since both parts were written as separate works, there may be some overlap between them. In this report, they are presented together to provide a complete overview of the project.

Delft University of Technology
5-10-2025
Ivo van den Enden

Abstract

Designing suspension systems for military terrain vehicles presents challenges due to conflicting performance requirements and demanding operational environments. This work applies a Systems Engineering V-Model approach to the tolerance-based redesign of a military terrain vehicle suspension. The project is part of the development of a new vehicle platform based on an existing prototype. The project begins with a literature review that compares suspension architectures based on key performance criteria, such as ride quality, wheel travel, ground clearance, and reliability. Based on this literature review, stakeholder needs, and user requirements, a double wishbone suspension is selected as the most suitable architecture for the new vehicle platform. To verify design requirements, a tolerance analysis is conducted to evaluate the effect of manufacturing tolerances on suspension angles, specifically camber and caster. A Python-based Kinematic model is developed to determine the effect of tolerances on the location of the suspension hardpoints. DynaTune-XL is used to simulate the suspension angles during wheel travel. The analysis shows that tolerances can be relaxed without exceeding predefined limits. Based on these insights, a redesign of the lower wishbone is made, focusing on manufacturability. The resulting redesign features a simplified geometry with a new shock absorber interface, optimized for production through sand casting followed by finishing machining. Material and process selection is done using Ansys Granta Edupack. The redesigned wishbone is verified through structural analysis using Altair SimSolid. The project demonstrates how the V-Model, commonly applied in aerospace and software development, can also effectively guide the development of suspension systems in the automotive/defense sector. In this work, the V-Model ensured full traceability from stakeholder needs and user requirements to verification, which helped translate high-level requirements into specific, verifiable suspension requirements. The introduced tolerance analysis method provided quantifiable insight into how dimensional variation in components led to variation in suspension angles during wheel travel. This demonstrated that the tolerances of the outer ball joints of the wishbones could be relaxed without exceeding predefined limits. The resulting lower wishbone redesign lays the foundation for transitioning from prototype to series production.

Contents

Part I

Literature Review

1

Evaluating Suspension Systems for Military Terrain Vehicles: A Comparative Analysis Based on Key Performance Criteria

1.1. Introduction

The suspension system in a wheeled vehicle consists of linkages, springs, and dampers that control the movement and forces between the wheels and the chassis of the vehicle. The suspension plays an important role in stability, safety, ride comfort, vehicle performance, and mobility. Military terrain vehicles must be capable of traversing rough terrain to complete their missions successfully. In these conditions, the suspension system has to isolate the vehicle body from vibrations of uneven terrain and maintain wheel contact with the ground to provide traction.

Designing a military terrain vehicle comes with many challenges; translating stakeholder needs into vehicle architecture is one of those challenges. There is a wide range of suspension systems available, and choosing the right system can be difficult. This literature review aims to provide a comparative analysis of suspension systems to aid vehicle architects in choosing the right suspension system for their military terrain vehicle. This leads to the research question associated with this literature review: *How do different suspension systems compare for use in military terrain vehicles based on key performance criteria?*
This research question is split into three sub-questions:
• *What key performance criteria for suspension systems in wheeled military terrain vehicles are identified in literature?*
• *What types of suspension systems for wheeled vehicles are described in literature?*
• *How are the identified suspension systems compared in the literature based on key performance criteria?*

1.2. Methods

This literature review follows the PRISMA methodology to ensure a systematic and transparent approach to identifying, selecting, and analyzing relevant studies.

1.2.1. Eligibility criteria

Literature is included or excluded according to the criteria listed below.

Inclusion criteria

- Studies focusing on suspension systems in military, terrain, off-road, or tactical vehicles.
- Research discussing key performance criteria in military terrain vehicles.
- Comparative analysis of suspension systems.
- studies comparing active and passive suspension systems.
- Fundamental books on suspension systems

Exclusion criteria

- Studies focusing on non-wheeled vehicles like tracked vehicles.
- Studies on suspension systems in planetary rovers or robots.
- Suspension optimization or tuning without comparison between different suspension systems.

- Research on control theory for (semi-)active and or active suspension systems.

1.2.2. Information sources
Relevant literature was collected from multiple sources to ensure complete coverage of the topic.

- Scopus
- SAE Mobilus
- Books
- Citation searching

1.2.3. Search strategy
A systematic search was conducted using Scopus and SAE Mobilus to collect relevant literature.

Scopus search query
```
ABS ( suspension OR wishbone OR mc AND pherson OR mobility )
AND ABS ( military OR terrain OR offroad OR tactical )
SUBJAREA ( engi )
AND NOT ( TITLE ( model OR rover OR robot OR learning OR tracked ) )
AND (
    LIMIT-TO ( EXACTKEYWORD , "Military Vehicles" )
    OR LIMIT-TO ( EXACTKEYWORD , "Automobile Suspensions" )
    OR LIMIT-TO ( EXACTKEYWORD , "Suspensions (components)" )
    OR LIMIT-TO ( EXACTKEYWORD , "Off Road Vehicles" )
)
AND ( LIMIT-TO ( LANGUAGE , "English" ) )
AND ( LIMIT-TO ( DOCTYPE , "ar" ) OR LIMIT-TO ( DOCTYPE , "cp" ) )
```

SAE Mobilus search query
```
(abstract_clean.stem: (Suspension OR Wishbone OR McPherson OR mobility))
AND (abstract_clean.stem:
(Military OR Terrain OR Offroad OR tactical OR "off-road" OR "off road"))
AND -(title.stem: (Track))
AND -(title.stem: (Learning))
AND -(title.stem: (Model))
```

1.2.4. Selection process
The first step in the selection process is to remove any duplicate studies from the search results. Next, titles and abstracts are screened to ensure their relevance to the topic. Full texts are then sought for retrieval. If the full text is inaccessible, the study is excluded. Finally, the remaining reports are assessed for eligibility through full-text screening using the previously defined inclusion and exclusion criteria.

1.2.5. Data collection process
Data is collected from the selected studies by reading the full-text papers and searching for data that can help answer the three sub-questions formulated in the introduction. Zotero reference management software is used to organize the studies.

1.2.6. Data items
The following data items are extracted from the selected studies:

- **Key performance criteria:** All performance criteria described in studies on suspension systems in military, terrain, off-road, or tactical vehicles were collected.
- **Comparative analysis:** Comparisons between different suspension types (e.g., independent vs solid axle or passive vs active) are collected.

- **Suspension system classification:** Information was collected on the types and configurations of suspension systems, including their applications, and advantages or limitations in military and off-road environments.

1.2.7. Synthesis methods

The collected data is synthesized to provide a comparative analysis of suspension systems and their performance in military terrain vehicles.

- All identified suspension systems are categorized based on suspension geometry (dependent, semi-dependent, independent). The spring and damper systems are classified into active, semi-active, and passive types. These categorizations are then organized into a **tree diagram**, to provide vehicle architects with a clear and structured overview of the available options for both suspension geometry and spring-damper configurations.
- An **overview table** was created to show which study discusses which suspension geometry and criteria, highlighting areas with existing research and identifying gaps where research is lacking. The table is structured with suspension geometries as columns and the identified criteria as rows. The cells in the table indicate which study discusses each suspension geometry and criteria.
- From the overview table mentioned above, the **comparisons of suspension systems** found in literature are grouped by performance criteria to show the strengths and limitations of different suspension systems. If present, comparisons between (semi-)active and passive systems are added to show the potential benefits or limitations of implementing (semi-)active systems.

1.3. Results

1.3.1. Study selection

The PRISMA flowchart in Figure 1.1 outlines the process of identifying, screening, and including studies. A total of 169 records were identified from databases, with 15 duplicate records removed, resulting in 154 records screened. An additional 7 records were found through websites and citation searching. 104 records were excluded during the screening process based on relevance. 50 reports were sought for retrieval, with 6 not retrieved due to access issues. After retrieval, 44 reports were assessed for eligibility from database sources, and 7 from other sources. 19 studies met the inclusion criteria and were selected for this literature review.

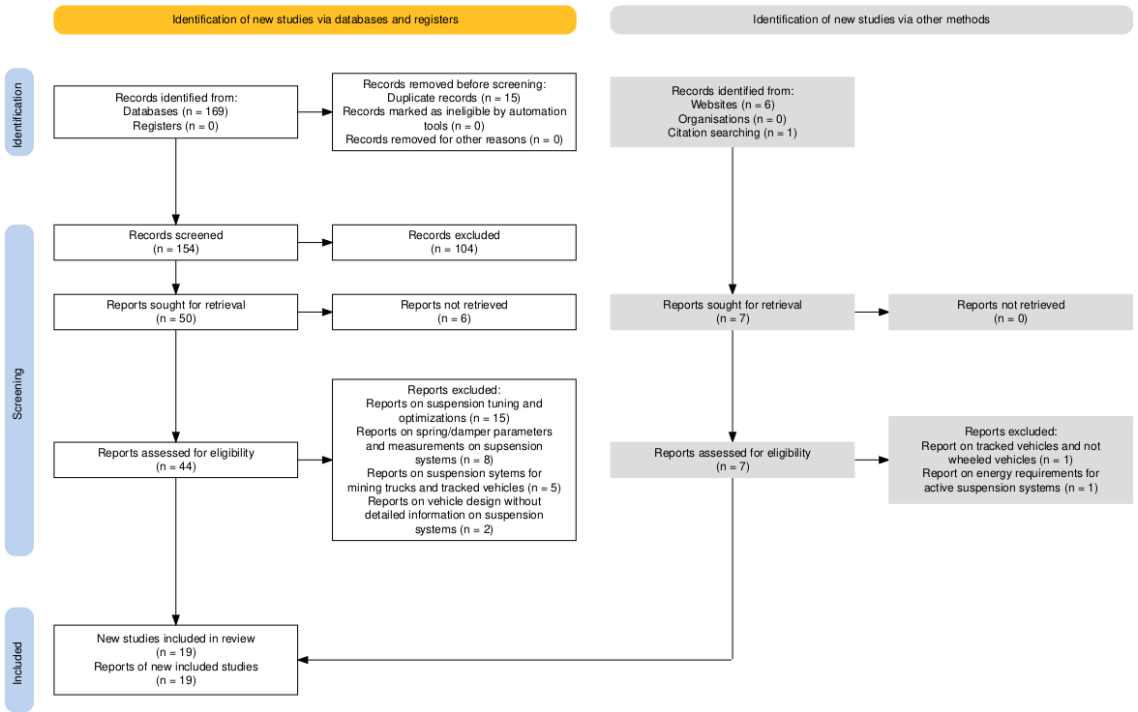

Figure 1.1: Prisma Flow diagram.

1.3.2. Key performance criteria

The following key performance criteria for military terrain vehicles are collected from the literature.

Off-road capability

• Ride quality: This refers to the vehicle's ability to absorb shocks and vibrations from uneven surfaces. Two tests on ride quality are commonly used: The maximum all-terrain-speed test and the shock absorption test. The first test determines the maximum vehicle speed at which the absorbed power to the base of the driver's spinal column reaches 6 W when driving over a root-mean-square surface roughness concrete washboard course set by ATPD 2131 guidelines. The shock absorption test determines the speed at which the vertical acceleration at the driver seat foundation exceeds 2.5g [1][2][3][4][5][6][7].
• Wheel travel and ability to twist: greater wheel travel and ability to twist help maintain tire contact with the ground, improving traction [6][8][9].
• Ground clearance: higher ground clearance improves off-road mobility by reducing the risk of bottoming out and maintaining traction in rough conditions. Military vehicles have large payload capacities; these payloads can affect the ground clearance depending on the type of suspension system [6][8][10][2][11].
• Body roll on slopes: the roll angle of the vehicle on slopes should be small to prevent the vehicle from tipping [3][8][12].

On-road capability

• Body roll when turning at high speeds: excessive body roll at high speeds can reduce stability and traction and increase the risk of rollover [2][3][4][6][8][10][12].
• Steering ability and wheel control: handling and minimizing unwanted steering inputs caused by obstacles or suspension movement [8].

Other considerations

• Reliability: to consistently perform under various operating conditions without failure [2][12][11].
• Costs [6].
• Package space: physical space allocated in the vehicle for integration of the suspension components [13][8].
• Vehicle bottom configuration and compatibility with armored hull: the suspension system affects the vehicle's height, center of gravity, and compatibility with blast protection [6][8].

Conflicting criteria

When designing suspension systems for off-road and on-road vehicles, there are inherent conflicts between the criteria for off-road and on-road capability. Off-road capability typically requires low spring rates, high wheel travel, and high ground clearance to maximize traction and ensure performance on uneven terrain. In contrast, on-road handling demands stiff springs and low ground clearance to improve roll stiffness and stability during higher-speed maneuvers. This creates a trade-off between having low roll stiffness for better cross-country performance and high roll stiffness for improved roll control at higher speeds.

1.3.3. Suspension systems overview

A suspension system overview is created by organizing all suspension types from the literature in a tree diagram in Figure 1.2. The suspension system consists of two main components, the suspension geometry and the spring-damper system. The suspension geometry can be classified into three categories: dependent, semi-dependent, and independent.

Dependent suspension: Both wheels are mechanically connected on the same axle, meaning movement in one wheel directly affects the other. Dependent suspensions are also called solid axle or rigid axle suspensions.

Semi-dependent suspension: There is some degree of connection between the wheels, but they still retain limited independent movement. An example is the torsion beam axle.

Independent suspension: each wheel moves independently without affecting the other. An example is the double wishbone and McPherson suspension.

The spring and damper system can be categorized as passive, semi-active, or active [1].
Passive suspension: A system containing only spring and damper elements and whose rates and forces cannot be varied by external signals. There is no means of adding external energy to the system [5].
Semi-active suspension: A system that contains no force actuators for inputting energy to the suspension system, but has the ability to vary the rate of energy dissipation within the suspension continuously. Typically, this involves the use of controllable dampers, which are modulated in some manner based on vehicle state [5].
Active suspension: A system containing force actuators (possibly in parallel with passive elements) that provides suspension forces according to some control law, which is a function of the vehicle state. Energy, usually a significant amount, may be added or taken out of the system [5].

Suspension systems often include a roll bar to limit roll angles and wheel travel. Roll bars can be added to dependent, semi-dependent, and independent suspensions. The addition of a roll bar makes an independent system behave more like a semi-dependent system. As with spring and damper systems, roll bars can be divided into passive and active categories.

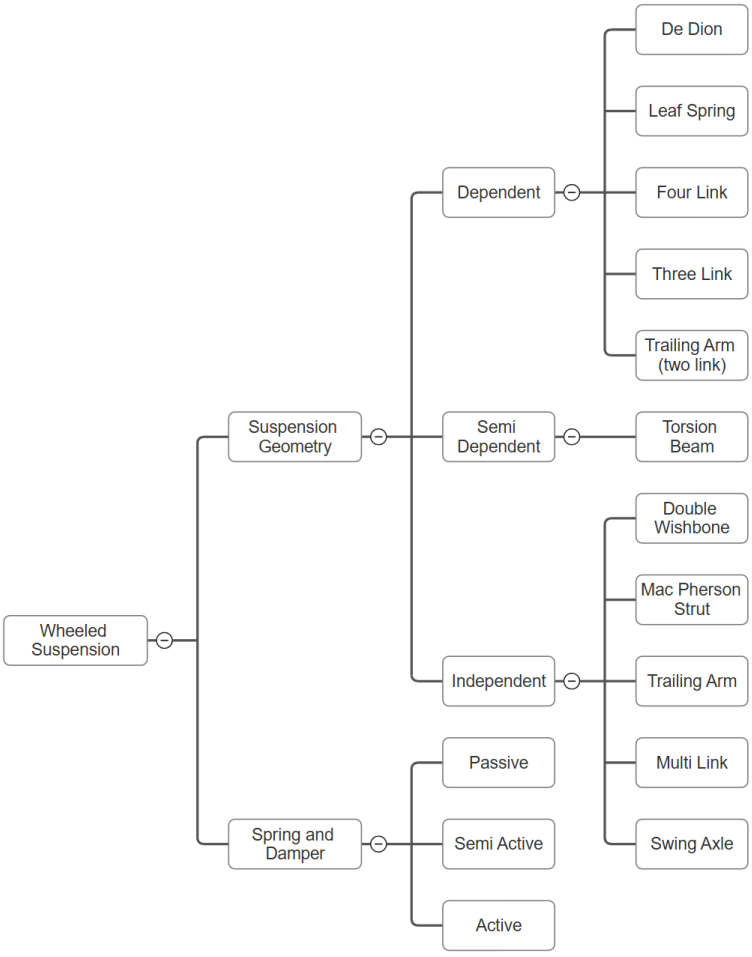

Figure 1.2: Overview of suspension systems, divided into suspension geometry and spring and damper systems. Based on [1][5][14][9].

1.3.4. Literature overview table

The collected literature comparing different suspension systems is summarized in Table 1.1, highlighting trends and gaps in the literature. The table is structured with the identified performance criteria on the vertical axis and the various suspension systems on the horizontal axis. Some papers discuss independent or solid axle suspensions in general without specifying particular geometries within these categories; these are included as general classifications in the table.

Criteria	Independent	Double wishbone	Solid Axle	Multi Link	Mc Pherson	Trailing Arm	Torsion Beam	Swing Axle
Ride quality	[6]	[7]	[6][7]					
Wheel travel / ability to twist	[6][13][9]	[8]	[6][8][13][9]					[8]
Ground clearance	[6][8][13]	[8]	[6][8][13]					[8]
Body roll on slopes and cornering	[6][9]	[8][7]	[6][8][7][9]					[8]
Steering ability and wheel control		[8][9]	[8][9]					
Reliability	[13]	[13]	[13][7][2]					
Costs	[6]		[6][7][9]		[15]			[15]
Package space		[15]			[15][14]	[14]		
Vehicle bottom configuration and compatibility with armored hull	[6][9]	[8]	[6][8][9]					

Table 1.1: Literature overview summarizing the evaluation of different suspension systems based on criteria across the identified studies. Independent and solid axle suspensions are included as broad categories since some papers discuss these suspensions in general, without specifying specific geometries.

1.3.5. Suspension system comparison per criteria

Ride Quality

In Crolla et al. [6], a six-wheel truck of 24 tonnes gross vehicle weight based on a crash tender design is used as an example to model an independent and solid axle leaf spring suspension using Vehicle Dynamics and Analysis Software (VDAS). The results of this study indicate that the independent suspension offers better vibration levels when traversing rough terrain, leading to better ride quality.
In Liao et al. [7], a M1078A1 full-time 4x4 truck with 2268 kg payload is tested with various suspensions installed. The M1078A1 was tested with five different suspension systems: 1. Baseline suspension, solid axle with leaf springs and passive shock absorber, 2. Oshkosh TAK4 independent double wishbone suspension with coil-over springs and passive shock absorber. 3. Meritor High-Mobility independent double wishbone suspension with coil-over springs and passive shock absorber. 4. Active shock solenoid valve, solid axle leaf spring with semi-active shock absorber. 5. Lord Magneto rheological solid axle leaf spring with semi-active shock absorber.

The ride quality is determined using concrete washboard courses of one and two inch RMS surface roughness, and the shock absorption test using 8 and 10 inch half-round single curb strikes [7].

For the off-road performance, the independent double wishbone suspension shows the most improvement. TAK4 shows a 105% increase in speed at the one-inch RMS washboard course and 25% increase in speed for the two-inch RMS washboard course compared to the baseline solid axle suspension. The Meritor HM double wishbone suspension achieves a 45% increase for one inch RMS and a 25% increase at two inch RMS. The solenoid valve and magneto rheological solid axle suspensions achieve 6 W ride speeds, which are 9% and 12% respectively more than the baseline solid axle suspension. For the shock absorption test, the TAK4 suspension achieves an 86% increase in speed on the 203 mm half-round and a 16% increase on the 254 mm half-round obstacle. The Lord MR has an increase in speed of respectively 32% and 30%. Those of the solenoid valve and magneto rheological suspensions are comparable with the baseline solid axle suspension [7].

Switching to an active or semi-active system can significantly improve ride quality. In Hayes et al. [2], an 8-ton LMTV/A1 truck with solid axle suspension with leaf springs was tested with passive dampers

and with electromechanical actuators as dampers. Testing on a washboard course with two-inch RMS surface roughness showed a 50% increase in maximum terrain speed when using the electromechanical dampers.

Ride quality is also affected by payload variations. Military terrain vehicles often have large payload variations, passive suspensions are optimized for a specific weight range, but significant payload variations can compromise the effectiveness of passive suspensions to maintain desired ride quality. LaPlante. [11] demonstrates that a semi-active suspension implemented in an HMMWV allows the vehicle to achieve similar absorbed power scores regardless of the weight trim of the vehicle.

Wheel travel and ability to twist

In Hohl. [8] A mathematical model is used to compare the kinematics of independent and dependent suspensions. Using this model, the maximum obstacle height is plotted against axle load distribution and spring stiffness for solid axle, swing axle, and double wishbone configurations. These plots show that solid axle suspension is superior in terms of wheel travel and twisting ability. The main reason for this is that the difference in wheel loads of two axles twisting in opposite directions is smaller in solid axles compared to independent suspension systems [9]. According to Crolla et al. [6], the wheel travel in traversing uneven terrain is dictated by the roll stiffness. Low roll stiffness allows the axle or wheels to move easily relative to the car body without large differences in wheel loads. Since the solid axle suspension generally has a lower roll stiffness, it performs better than independent suspension in terms of wheel travel on uneven terrain [6]. Kline [13] also describes limited wheel travel as one of the disadvantages of independent suspension compared to solid axle suspensions.

In passive systems, the roll stiffness is set as a compromise between wheel travel in uneven terrain and body roll in high-speed maneuvering. Active systems can change roll stiffness to accommodate different operating conditions [16].

Ground clearance

Rigid axles maintain constant ground clearance regardless of payload variations, but the differential housing, as the lowest point, can become an obstacle on uneven terrain. In contrast, independent suspensions experience ground clearance changes with payload variations but allow for a flat vehicle underbelly, free from obstructing axle beams. On uneven terrain, a flat underbody reduces the risk of getting stuck compared to a rigid axle's differential housing, potentially improving off-road performance [8].

Crolla et al. [6] state that independent suspensions have poorer ground clearance than solid axle suspensions because their ground clearance is affected by normal suspension movement, while ground clearance in solid axle suspensions is essentially constant. Kline [13] agrees with Crolla et al. [6] and lists ground clearance as limited in independent suspensions compared to solid axle suspensions.

Implementation of active or semi-active systems enables functionalities such as terrain-dependent ground clearance [10]. In LaPlante. [11] a semi-active suspension is implemented in a M1113 HMMWV. The semi-active system allows the HMMWV with independent double wishbone suspension to maintain constant ground clearance despite significant variations in payload.

Body roll on slopes and when cornering

Crolla et al. [6] state that the body roll of a vehicle depends on the roll center and roll stiffness of the suspension. The roll center of a solid axle with leaf springs is relatively high at the height of the spring hangers, but is difficult to change. For independent suspensions, the roll center is generally lower but allows for more design freedom by changing the geometry of the control arms. Shifting the roll center too high in an independent suspension can lead to jacking and vehicle instability. The roll stiffness in independent suspensions is generally higher than in solid axle suspensions. Crolla et al. [6] conclude that both independent and solid axle configurations can have similar body roll depending on design parameters.

Hohl. [8] uses a mathematical model to plot roll angle versus suspension system, considering different axle load distributions and different spring rates. The resulting graph shows that swing axle suspensions have the lowest roll angles, followed by double wishbone suspension and lastly solid axle suspension [9].

In Liao et al. [7] a M1078A1 full-time 4x4 truck with 2268 kg payload is tested with various suspensions installed, Solid axle with leaf springs and passive shock absorber, Oshkosh TAK4 independent double wishbone suspension with coil-over springs and passive shock absorber, Meritor high mobility independent double wishbone suspension with coil-over springs and passive shock absorber, Active shock solenoid valve solid axle leaf spring with semi-active shock absorber and Lord Magneto rheological solid axle leaf spring with semi-active shock absorber. These suspensions are tested in a circular steer test, double lane change test, and sinusoidal steering test.

For the circular steer test, each vehicle's maximum speed is recorded prior to wheel lift. The M1078 with Oshkosh double wishbone suspension achieves the highest average speed (46.5 km/h) and lateral acceleration (0.47g), maintaining roll angles 2.7° above baseline. The MR solid axle vehicle reaches 45.2 km/h and 0.43g but experiences premature outrigger touchdown due to excessive 10.9° body roll. The SV solid axle and Meritor HM double wishbone underperform, with maximum speeds 1.5 km/h and 0.5 km/h below baseline [7].

Double-lane-change testing is conducted by determining the maximum velocity at which the vehicles can successfully traverse the course. The MR solid axle vehicle achieves the highest average speed at 76.6 km/h (9.4% above baseline). The Meritor HM double wishbone and SV solid axle follow closely at 73.5 km/h and 72.7 km/h, both about 5% above baseline. The Oshkosh double wishbone reaches 72.3 km/h, a 3.3% increase [7].

A sinusoidal steering test is done to determine the highest acceleration without wheel lift or outrigger touch. The Oshkosh double wishbone achieves the highest lateral acceleration (0.52g), followed by the Lord MR solid axle (0.49g) and the SV solid axle (0.48g). Meritor HM double wishbone and the M1078 baseline solid axle perform similarly at 0.46g [7].

Contrary to passive systems, (semi-)active systems can adjust the roll stiffness to accommodate various operating conditions [10]. In Hayes et al. [2], an 8-ton LMTV/A1 truck with solid axle suspension with leaf springs was tested with passive dampers and with electromechanical actuators as dampers. The vehicle with a passive solid axle suspension rolled two to three degrees during slalom testing, while the vehicle equipped with the electromechanical actuators exhibited no measurable roll.

Beno et al. [12] demonstrated with simulations that active suspension systems can significantly reduce the likelihood of rollovers on slopes due to road breakaway for MRAP/JLTV class vehicles. This is achieved by pushing (extending) on the downhill side of the vehicle and pulling inward (retracting) on the uphill side.

Khalil et al. [17] simulated the effect of using no anti-roll bar, a passive anti-roll bar, and an active anti-roll bar for off-road vehicles to prevent rollover at high speed on smooth roads. Simulation results show that adding an anti-roll bar decreases body roll angle, with active anti-roll bars providing the most effective roll control. The active anti-roll bar system reduces the maximum rolling angle by more than 95% in all tests compared to its counterparts.

Steering ability and wheel control

A disadvantage of solid axle suspension is the gyroscopic moment, which negatively impacts steering precision and wheel control. When one wheel crosses a hump, it creates a vertical displacement relative to the chassis. The wheels experience simultaneous displacement in roughly equal and opposite directions relative to the chassis. Since rotating wheels function as gyroscopes, this induced gyroscopic motion tends to make the steerable wheels rotate around their kingpins [9].

Another drawback of a rigid axle design is its higher unsprung mass compared to independent suspension systems. This becomes problematic when both wheels encounter an obstacle simultaneously, as the entire axle's mass is engaged in the movement [8].

Reliability

Kline et al. [13] state that independent suspensions are less robust than solid axles. However, designers have pushed the limits of independent suspension in terms of durability, as shown in the military Humvee, which features independent front and rear suspension. Liao et al. [7] list durability in high load environments for off-road applications as one of the advantages of solid axle suspensions compared to independent systems. Hayes et al. [2] further add that solid axles with leaf springs provide the army with an ultra-reliable and robust suspension system.

LaPlante. [11] tests replacing passive suspension in an up-armored HMMWV with semi-active suspension. The up-armored HMMWV often exceeds its design weight by 25%, leading to reduced reliability and frequent suspension failures. Overloading the vehicle leads to limited compression travel, causing severe bottoming and transmission of high shock loads to the suspension and chassis. Semi-active suspension can reduce bottoming out and therefore has the potential to increase reliability compared to the passive suspension currently used.

Costs

Solid axle suspensions rely on inexpensive, well-proven technology, whereas equipping a vehicle with independent suspension comes at a higher cost [6]. Hohl. [9] explains that solid axles remain popular in off-road vehicles partly because they are cost-effective, as they can be easily adapted from standard commercial trucks.

Bucchi et al. [15] describe swing axle suspension as inexpensive, similar to the widely used low-cost McPherson suspension in passenger car front axles. In contrast, Hohl. [8] argues that swing axles require specialized designs with few commercial components and further adds that the axle-differential connection is complex and expensive. (Semi-)Active suspensions come with a significantly higher cost than passive systems due to the additional components required, such as sensors, actuators, and electronic control systems.

Package space

Package space is a critical factor in suspension system design. The McPherson suspension offers a compact package size, leaving more room for the engine in front-engine vehicle configurations. Double wishbone suspensions typically require more space to fit the upper A-arm [15]. The trailing arm suspension allows for a compact layout in rear suspension configurations [14]. Ultimately, the compatibility of a suspension system with a vehicle's design depends on the available package space, with the choice of suspension type being influenced by the overall design and intended use of the vehicle.

Vehicle bottom configuration and compatibility with armored hull

The bottom configuration of a vehicle influences the overall vehicle height, the height of the center of gravity, and the compatibility with blast protection features such as an armored hull. An advantage of independent suspension is that the body or chassis can be positioned between the suspension and wheels, allowing for a lower vehicle profile. In contrast with a solid axle suspension, the chassis and body must be positioned above the axle, resulting in a higher overall vehicle height [6].

Figure 1.3 found in Hohl. [8] illustrates the difference in vehicle bottom configuration of an independent double wishbone and a dependent solid axle suspension. From the figure, the effect on overall vehicle height and height of the center of gravity of the chosen suspension is clearly visible. The independent configuration also has the added benefit of being enclosed in the armored hull and is therefore less prone to damage by obstacles or underbelly blasts.

1.4. Discussion

1.4.1. Summary of key findings

Ride quality

Regarding ride quality, experimental testing and simulations from multiple studies indicate that independent suspensions such as the double wishbone suspension outperform solid axle suspension when it comes to ride quality. Literature also shows that (semi-)active systems can increase ride quality for both independent and dependent suspensions when compared to passive systems.

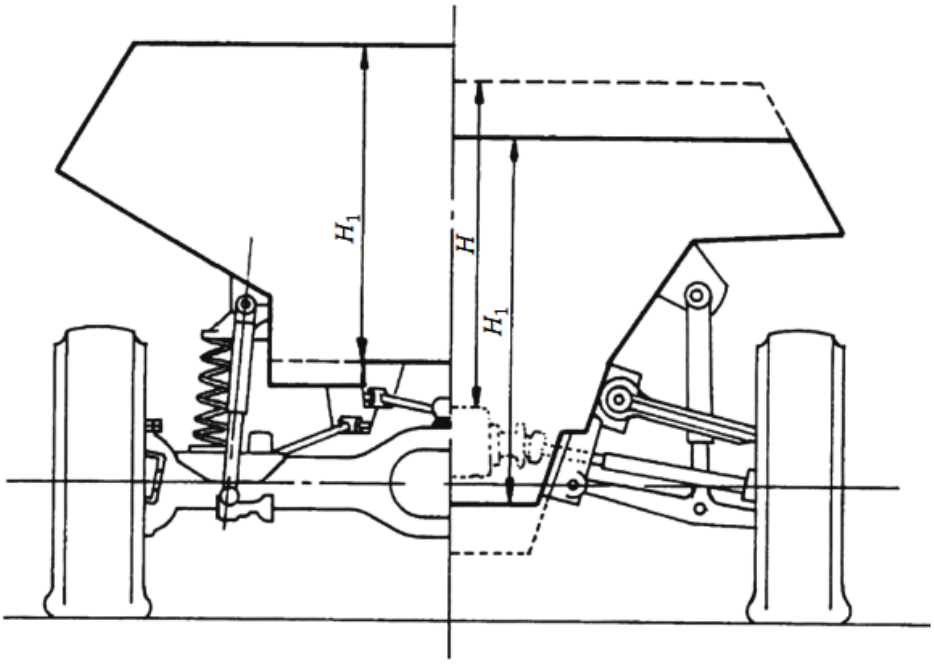

Figure 1.3: Armored vehicle with V-hull with independent and non-independent suspension [8].

Wheel travel and twisting ability

Solid axles perform better than independent systems when it comes to wheel travel and twisting ability mainly because the difference in wheel loads is smaller and in general roll stiffness is lower in solid axle suspensions compared to independent suspensions. Implementation of (semi-)active systems enable adjustable roll stiffness, which can have positive effects on wheel travel and ability to twist.

Ground clearance

When it comes to ground clearance both independent and dependent suspensions have their advantages and disadvantages. Dependent suspensions have a constant ground clearance that is unaffected by payload variations, but have differential housings as the lowest point under the vehicle which can become an obstacle on uneven terrain. In independent suspension the ground clearance is affected by payload variations, but a flat underbody is possible, which reduces risk of getting stuck. With (semi-)active systems the ground clearance can be varied depending on the terrain.

Body roll

Body roll depends on roll center height and roll stiffness, independent suspension allow for more design freedom in setting roll center height. Roll stiffness can be made the same on both independent and dependent suspensions depending on design parameters. A big advantage of active suspension for body roll is the ability to change the roll stiffness to accommodate varying operating conditions.

Steering ability and wheel control

When it comes to steering ability and wheel control, dependent suspensions have some disadvantages, they can have undesirable steering caused by gyroscopic forces and have more unsprung weight when compared with independent suspensions.

Other considerations

Solid axle suspensions are considered to be more robust and reliable compared to independent suspensions. (semi-)active systems have potential to increase reliability by decreasing high forces and shocks in suspension components, it is however unclear if the added components and complexity of these systems result in an overall increase or decrease of reliability. Solid axles are considered the most inexpensive since they are adapted from commercially available options, independent suspension tend to be more expensive, and addition of (semi-)active systems adds considerable costs. Package space

and bottom configuration are other important considerations. In armored vehicles with underbody protection independent suspensions are preferred since they result in a lower overall vehicle height, lower center of gravity and can be partly enclosed by the protective hull.
Other considerations that are worth considering when comparing suspension architecture are:
• Max steering angle
• Compatibility with 4-wheel steering
• Compatibility with hub reduction
These points are obtained from the industry but were not found in the obtained literature.

1.4.2. Literature trends and gaps

The pattern in Table 1.1 suggests that multi-link, McPherson, torsion beam, trailing arm, and swing axle suspensions are rarely or never discussed in military terrain vehicle literature, while the use of solid axles and independent double wishbone suspensions is well documented. Possible explanations for this are listed below:
Multi-link suspensions have many moving parts which makes them quite complex. These types of suspensions are typically used in vehicles where precise handling is prioritized over durability and simplicity. Their complexity makes them less suitable for military terrain vehicles.
McPherson suspensions lack sufficient wheel travel and robustness for heavy off-road applications.
Trailing arm suspensions provide less wheel travel compared to solid axles or double wishbone suspensions. **Torsion beam** suspensions have insufficient wheel travel and strength making them unsuitable for military vehicles. **Swing axle** suspensions suffer from extreme camber change during suspension travel, leading to instability on rough terrain. **Solid axle** suspensions have a long history in military vehicles, dating back to early off-road trucks and jeeps, due to their rugged simplicity and reliability. **Double wishbone** suspensions offer better structural strength than other independent suspension types, making them more suitable to handle the high stresses of military terrain use.

1.4.3. Limitations of results

The findings of different studies vary due to differences in methodologies, assumptions, and test conditions. Some studies rely on mathematical models or simulations, while others use experimental testing. Simulations allow controlled comparisons but may oversimplify real-world complexities, while experimental tests provide realistic data but are limited to specific vehicles and test conditions. The type of vehicles used in the study also introduces variability. An example is the difference between the M1113 HMMWV and the bigger M1078A1 truck that are used in some studies. The use of different vehicles of different weight classes can lead to different results, making direct comparisons difficult. These limitations make it important to critically assess the context of each study and avoid overgeneralizing findings.

1.4.4. Limitations of process

This review follows the PRISMA method to ensure a systematic approach; however, some limitations remain. The search query was developed after an initial exploration of the research field and the identification of relevant keywords. Nevertheless, some studies may have been excluded due to variations in terminology or limited accessibility. Additionally, the niche nature of military terrain vehicle suspension research means that available literature is scarce, which increases susceptibility to bias in study selection and results.

1.4.5. Future work and implications for practice

In future military terrain vehicles, hybrid or electric powertrains are being considered due to potential advantages in reducing environmental impact and enhancing stealth capabilities through silent operation. In this context, (semi-)active suspensions offer additional benefits, such as the regenerative ability of suspension travel [18] and the reduction of rolling losses [19], further improving efficiency and mobility. However, further research is needed to evaluate the durability, reliability, and energy efficiency of such systems in extreme off-road conditions.

For vehicle architects, there is no universal suspension solution that is optimal for all operating conditions. The choice of suspension architecture must be guided by the specific operational requirements of the vehicle, including factors such as mobility, durability, payload capacity, terrain type, and mission

profile. Conflicting requirements often lead to trade-offs, making it essential to prioritize key performance aspects based on the vehicle's intended use.
Passive suspension systems will always involve a compromise between on-road and off-road performance, as they cannot dynamically adapt to changing terrain conditions. (Semi-)active suspension systems can help mitigate this trade-off by adjusting damping, stiffness, and ride height in real time, however they introduce additional complexity, cost, and maintenance considerations.

Part II

A Systems Engineering V-Model Approach to the Tolerance-Based Redesign of a Military Terrain Vehicle Suspension

2

Introduction

The suspension system plays an important role in stability, safety, ride comfort, vehicle performance, and mobility. Especially for military terrain vehicles that must be capable of traversing rough terrain to complete their missions. In the defense and aerospace sector, the development of complex systems is typically structured using the Systems Engineering V-Model. Originally, the V-Model was developed for the design of complex mechatronic defense systems [20]. The V-Model approach ensures a structured workflow, where each design step is paired with a corresponding verification step. In the automotive industry, tolerance analysis plays an important role in ensuring design robustness. Small geometric variations in suspension components can significantly affect parameters such as camber, caster, and toe. To address this, tolerance analysis is routinely applied during development to predict how manufacturing variation propagates to vehicle-level performance.

As part of a new project, a military vehicle platform will be developed based on an existing prototype vehicle. At the outset of such a project, a key challenge is determining whether the prototype suspension architecture is suitable for further development or whether alternative concepts provide a better foundation. The current double wishbone suspension of the prototype fulfills its functional role but was built with very tight tolerances, which made it costly and unsuitable for series production. This motivates a redesign of the suspension to improve manufacturability and a consideration of the current tolerances in the suspension system. From a methodological perspective, the project is also an opportunity to apply the Systems Engineering V-Model to the redesign of a mechanical subsystem. In the defense sector, accountability and verification are essential, making the V-Model a natural choice to structure the process from stakeholder needs to verification. However, while its use is well-established in aerospace and software/electronics within the automotive industry, applications to mechanical systems, such as vehicle suspensions, remain under-reported. This raises both a challenge and an opportunity: to assess the value of the V-Model for guiding a practical redesign and ensuring traceability in a defense engineering context.

In this project, the V-Model is applied as the overarching framework for the suspension redesign process. The aim is to advance the development of a military vehicle suspension from prototype to series production. This involves structuring requirements and verification activities through the V-Model, conducting a tolerance analysis to determine where tolerances can be relaxed without compromising performance, and redesigning the lower wishbone to improve manufacturability while maintaining compliance with functional requirements. This work makes three main contributions:

A case study demonstrating the use of the V-Model as a framework for suspension design in the automotive and defense context.

A tolerance analysis linking manufacturing tolerances to variation in suspension angles.

A redesign of the lower wishbone that incorporates both system requirements and manufacturing considerations.

The report is structured to follow the steps of the Systems Engineering V-Model. Chapter 3 presents the methods and results. It begins with defining stakeholder needs and user requirements, and translating them into system-level requirements, followed by the selection of a suitable suspension architecture. The chapter continues with the tolerance analysis, where suspension component tolerances are linked to variations in suspension angles. Based on these insights, a redesign of the lower wishbone is developed and verified through structural analysis.

Chapter 4 discusses the outcomes, evaluating the use of the V-Model approach and reflecting on the tolerance analysis. Implications of the redesign choices and the structural analysis method are also discussed.

Chapter 5 concludes the report by summarizing the key results, contributions, and implications. Supporting material is presented in the Appendices.

3

Methods & results

This chapter describes the methodology and results of the suspension design process, structured according to the systems engineering V-Model as shown in Figure 3.1. The definition of requirements (Section 3.1), suspension architecture selection (Section 3.2), and the lower wishbone redesign (Section 3.4) all correspond to the left side of the V-Model. The right side of the V-Model covers the verification, including the tolerance analysis linked to suspension angles (Section 3.3) and structural verification of the redesign (Section 3.5). In this way, each step of the process can be traced back to stakeholder needs and user requirements, while ensuring that the final subsystem design is validated against the intended functionality. Section 3.1 begins with the definition of requirements, which corresponds to the upper left block of the V-Model.

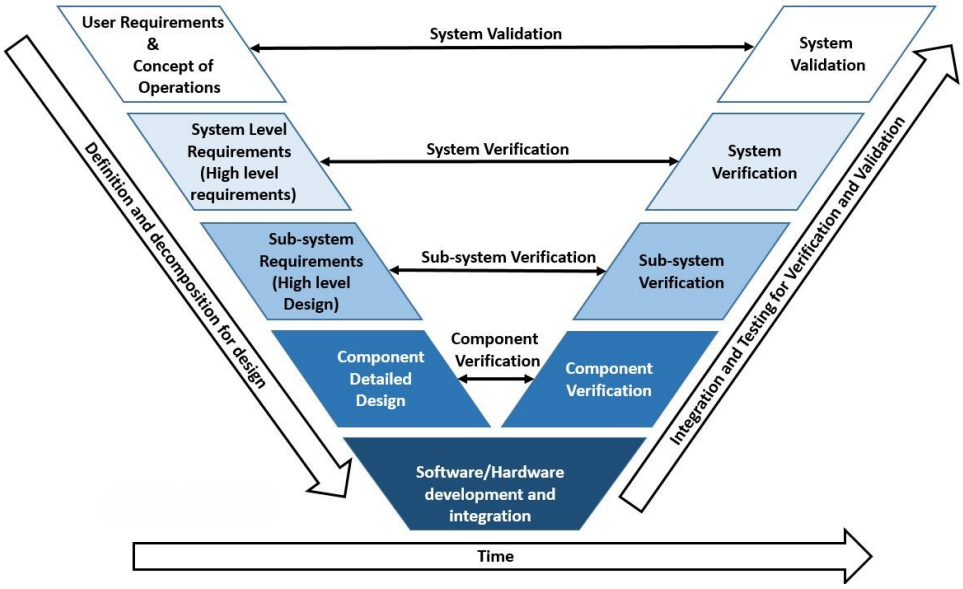

Figure 3.1: Systems engineering V-Model [21].

3.1. Definition of requirements

The first step in the V-Model is to define the user requirements and user scenarios; based on these, the system-level requirements can be formulated. In this case, only the requirements that affect the vehicle suspension are taken into account. Table 3.1 shows the user scenarios and stakeholder needs translated into specific requirements for the suspension system of the vehicle. The right column of the table shows how each of the requirements will be verified, corresponding to the right side of the V-Model.

ID	User scenarios and Stakeholder needs	System level requirements	Verification of requirement
R1	Use existing knowledge and reduce development cost by reusing the center spine chassis	Suspension shall be compatible with the center spine chassis	Integration check in CAD model
R2	Vehicle operational mass is between 8-10 tonnes to support sufficient payload capacity	Suspension shall support and safely operate within a vehicle gross weight range of 8-10 tonnes	Load case analysis using FEA
R3	Vehicle shall be transportable in a 20-foot ISO container	Suspension track width and integration shall ensure overall vehicle width $\leq$ 2.15 m	Dimensional verification in CAD model
R4	Vehicle should be capable of operating across a variety of terrains to complete its missions	Suspension design shall enable: • Static tilt angle $\geq$ 32.9° • Ground clearance $\geq$ 0.35 m • Break-over angle $\geq$ 31° • Approach and departure angles $\geq$ 40.5°	Kinematic analysis, static stability test, physical testing on vehicle proving grounds
R5	The vehicle must maintain stable handling and mobility during missions, ensuring safety and effectiveness even when manufacturing tolerances introduce variation in suspension geometry	Suspension geometry shall ensure a maximum statistical variation due to manufacturing tolerances in camber and caster angles compared to the nominal values of: • Camber angle $\pm$ 0.45° • Caster angle $\pm$ 0.65°	Tolerance analysis to verify suspension angle variations under manufacturing tolerances
R6	Vehicle shall be capable of operating in extreme cold climates without loss of structural integrity in suspension components.	Suspension components, especially those exposed to impacts on the vehicle's underside, shall demonstrate sufficient impact toughness by absorbing $\geq$ 27 J in a Charpy V-notch test performed at $-46\,^{\circ}\mathrm{C}$.	Material certification and Charpy V-notch impact testing at $-46\,^{\circ}\mathrm{C}$.

Table 3.1: Traceability of requirements from stakeholder needs to system-level requirements and verification.

3.1.1. Additional requirements and considerations

After the suspension architecture was selected (Section 3.2), the company specified that the existing press-fit bearing interface between the chassis and wishbones must be retained. This constraint was not present in the initial user requirements but was introduced following the architecture decision. As a result, this interface was excluded from tolerance relaxation and redesign considerations. In terms of the V-Model, this represents a step back up the left leg from high level design to system level requirements.

In the current prototype, the lower wishbones were designed to be interchangeable across all four corners of the vehicle. This choice simplifies spare part management but requires corner-specific bushings. While this interchangeability is not an initial requirement, it is reconsidered during the redesign phase of the lower wishbones.

3.2. Suspension architecture selection

Based on the system-level requirements defined in section 3.1 and the findings of the literature review in Chapter 1, a suitable suspension architecture can be selected for the new vehicle platform. This section corresponds to the middle left leg of the V-Model, the high-level design phase.

Three suspension architectures are considered based on the findings of the literature review from Chapter 1 and a market analysis provided in Appendix C:

- **Double wishbone** suspension
- **Solid axle** suspension
- **De Dion** suspension

These three suspension architectures can be evaluated against the system-level requirements from section 3.1. Requirements R1–R4 primarily govern the selection of the suspension architecture, as they directly relate to chassis compatibility, vehicle mass, dimensional constraints, and vehicle mobility, which are the most critical factors for the suspension design. A requirement matrix with the three considered suspension architectures is included in Appendix C.

3.2.1. R1 - Compatibility with center spine chassis

Double wishbone suspension is proven to be compatible with a center spine chassis; example vehicles of this compatibility are GRF, Mammoth, and the Ocelot Foxhound. For the solid axle and the De Dion axle, no examples of compatibility with a center spine chassis are found. While the integration is probably possible, it will result in an overall higher vehicle since the solid axle and De Dion axle need room to articulate under the chassis.

3.2.2. R2, R3 - Vehicle mass and dimensional constraints

Achieving a maximal vehicle width of 2.15 m and a vehicle mass of 8-10 tonnes is possible with the double wishbone suspension and the De Dion axle. The current vehicle prototype (double wishbone) and the GDELS Mowag Eagle V (De Dion) are examples of this. Finding a commercially available solid axle that meets both the weight demands of an 8–10 tonne vehicle and fits within the 2.15-meter track width limit has proven quite challenging, and so far, no existing axle has been found that fulfills both requirements.

3.2.3. R4 - Vehicle mobility

For the mobility requirements, the static tilt angle and the ground clearance are affected by the suspension system. All three considered suspension architectures can meet the ground clearance requirement, and as such, this requirement does not influence the architecture selection. The static tilt angle depends on the track width, the height of the center of gravity, the height of the roll center, and the roll stiffness of the vehicle. Given the requirement of vehicle width < 2.15 m, that leaves three variables that affect the static tilt angle.

Height of center of gravity: In combination with a center spine chassis and the same ground clearance for all architectures, the overall height of the chassis and vehicle will be greater in a solid axle and de Dion suspension compared to a double wishbone. A solid axle and De Dion axle need room below the chassis to articulate, effectively raising the COG of the vehicle as illustrated in Figure 3.2.

Roll center height: In general, the roll center height of a solid axle and de Dion is higher (at axle center) but difficult to alter; the roll center height of a double wishbone is generally lower but can be altered by changing the control arm geometry.

Roll stiffness: Roll stiffness is generally higher in double wishbone suspension, but it can be made the same for all three architectures.

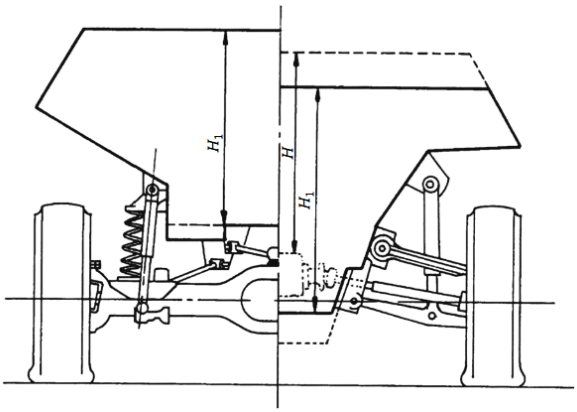

Figure 3.2: Vehicle height comparison between solid axle and double wishbone suspension [8].

Based on the evaluation of the system-level requirements R1-R4, the double wishbone suspension architecture is identified as the most suitable option for the new vehicle platform. It satisfies the chassis compatibility, mass, dimensional, and mobility requirements and provides flexibility to position the roll center. The solid axle and De Dion architectures lack proven compatibility with a center-spine chassis and impose constraints on vehicle dimensions and center of gravity height.

3.3. Tolerance analysis

With the double wishbone suspension architecture selected in Section 3.2, the next step in the V-Model is to verify whether this configuration can meet requirement R5 regarding the variation in suspension angles due to manufacturing tolerances. This stage corresponds to the subsystem verification level on the right side of the V-Model.

A tolerance analysis is used to perform this verification. Tolerance analyses show how manufacturing and assembly tolerances affect the functional performance of a system. In a vehicle suspension system, these tolerances can affect the position of the suspension hardpoints, which in turn affect suspension angles and kinematic behavior. These are important parameters for the vehicle's handling, ride quality, and stability.

Several methods are used in the literature to assess the impact of manufacturing tolerances on vehicle suspension. A standard practice is the process of using DOE (Design of Experiment) optimization [22]. In the field of tolerance analysis, DOE systematically varies suspension dimensions or hardpoint locations within their tolerance range and evaluates the resulting changes in functional performance of the suspension system. This makes it possible to identify the most critical tolerances and quantify their effect on the suspension system. Another method used by Rotundo et al. [23] and Lanzavecchia et al. [24] is a Monte Carlo DOE approach using computer-aided tolerancing (CAT) software. The CAT software enables tolerance chains to be established directly from CAD assemblies, utilizing component models with specified tolerances. Monte Carlo simulations are used to randomly vary input parameters, producing statistical distributions of output variables and thereby assessing the probability that performance requirements are met. Kim et al. [25] extended this approach by incorporating multibody elastokinematic analysis, while Borisenko et al. [26] applied multibody simulation in MSC Adams, using variations in hardpoint coordinates as inputs. Because a complete exploration of mutual displacements in all directions would require more than one billion simulations, Borisenko et al. focused on the hardpoints most susceptible to displacement during production and assembly.

The method used in this work combines elements from the approaches described in the literature. Since CAT software was not available, a kinematic suspension model was developed in Python to evaluate the kinematic state of the suspension based on component tolerances. Following the idea of Borisenko et al. [26], the analysis focuses on a limited set of scenarios rather than considering all possible displacements in every direction, which would require a large number of simulations. The method is applied to the double wishbone suspension of the prototype vehicle, with the specific aim of relating component tolerances to variations in suspension angles. The scope of the analysis is restricted to

manufacturing tolerances in the chassis, the chassis–wishbone interfaces, and the wishbones themselves. Ball joints and bearings are considered ideal, with no play. Both the chassis and wishbones are treated as perfectly rigid bodies with no compliance or deformation. The upright (wheel knuckle) is excluded from the analysis because it is manufactured to very tight tolerances, making its influence on camber minor compared to the tolerance chains leading to the outer ball joints of the wishbones. Furthermore, the caster angle is independent of upright tolerances since it is defined by the steering axis through the outer ball joints of the wishbones.

The first step is to extract the suspension hardpoint coordinates from a CAD model. Secondly, the tolerance chains to each of these hardpoints are established using component tolerances. With these tolerance chains, a kinematic model can be made that plots the suspension hardpoints based on the part tolerances. The output of this model can then be used to plot the suspension angles during wheel travel. After which, the nominal suspension angles can be compared to the suspension angles affected by tolerances. The designer specified variation in suspension angles, requirement R5 from table 3.1 can then be verified, and hardpoint tolerances that can be relaxed or tightened can be identified.

3.3.1. Tolerance chains

The double wishbone suspension is a mechanical sub-system consisting of multiple components, each of which has its own dimensional tolerances. Tolerances describe the allowable variation of a dimension from its nominal value. This study assumes that all tolerances follow a Normal Probability Density Function, with each dimensional tolerance defined as three times the standard deviation [23] (Figure 3.3). The double wishbone suspension can be represented as a set of suspension hardpoints connected by linkages, as illustrated in Figure 3.4. The equivalent tolerance of the suspension hardpoints can be determined by making tolerance chains to each of these hardpoints.

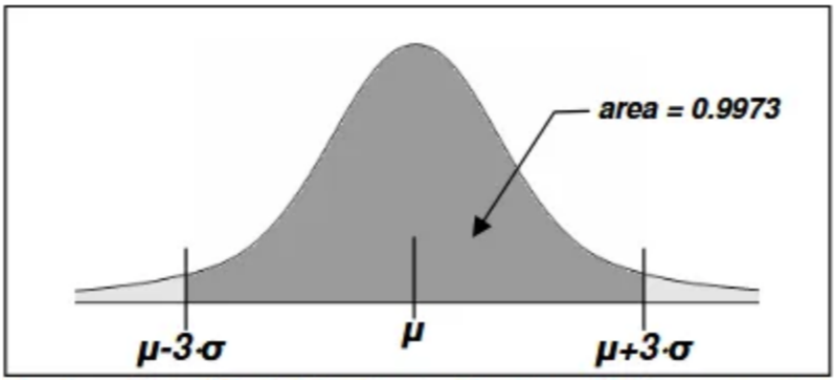

Figure 3.3: Normal Probability Density Function. μ is the mean value, σ the standard deviation. The tolerance value $\pm$T corresponds to $\pm 3\sigma$ [23].

A **tolerance chain** is formed by combining the tolerances of individual components to evaluate the overall variation of a critical assembly dimension. In the **linear (worst-case) method**, all tolerances in the chain are assumed to accumulate in the most unfavorable way. This guarantees compliance but can be overly conservative [27]:

$$T_{\text{total}} = \sum_{i=1}^{n} T_i$$

The **statistical method** assumes that each part's variation from nominal is random and independent, following a normal distribution, which gives a more realistic estimate [27]:

$$T_{\text{total}} = \sqrt{T_1^2 + T_2^2 + \cdots + T_n^2}$$

In this analysis, both the worst-case and the statistical methods are used. The tolerance chain of the suspension hardpoints is defined in three dimensions (x, y, z) relative to a predefined datum on the vehicle chassis. The chain includes the accumulated tolerances resulting from GD&T data of the chassis,

the interface between the chassis and wishbones, and the tolerances of the wishbones themselves. The positions and tolerances of the suspension ball joints (U3 and L3) are defined relative to the interface points (U1-U2, L1-L2). This ensures that the tolerance chain follows a logical order from the chassis to the interface points and finally to the ball joints on the wishbones. Table 3.2 shows the tolerances for each point using the linear (worst-case) and statistical methods. The inner hardpoint positions and tolerances are defined in a reference system linked to the SolidWorks model of the suspension. The positions and tolerances of the suspension ball joints (U3 and L3) are defined in local reference systems that rotate around the axes through their respective interface points (U1-U2 and L1-L2). Each local reference system is based on the plane spanned by the interface points (U1-U2 and L1-L2) and the ball joint itself. Because the ball joints lie in these planes by definition, they cannot deviate in the perpendicular (Z) direction. Therefore, no tolerances are assigned in Z, only within the plane directions (X and Y).

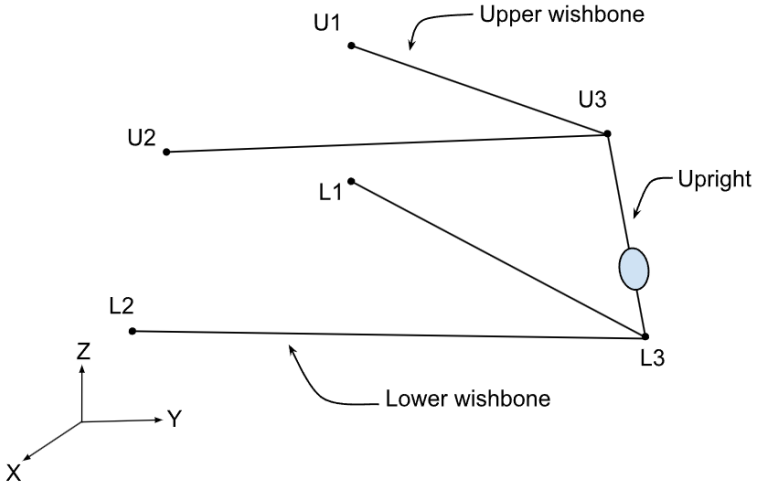

Figure 3.4: Schematic drawing of the double wishbone suspension, U1-U3 and L1-L3 are the suspension hardpoints.

3.3.2. Kinematic suspension model

To plot the suspension angles of the vehicle, we need the positions in space of all the suspension hardpoints with their tolerances included. Each of these hardpoints has tolerances in XYZ dimensions as shown in Table 3.2. When considering only the outer bounds, i.e., each axis can be at either the lower or upper bound of its tolerance. This results in $2^3 = 8$ possible locations for one hardpoint. For all six hardpoints, there would then be $8^6 = 262144$ possible kinematic states for the suspension. In this work, it is proposed to assess only the scenarios that have the most significant effect on the variation in camber and caster angles. Camber is the inclination of the wheel in the lateral (Y–Z) plane, where positive camber means the top of the wheel tilts outward and negative camber means it tilts inward. Caster is the inclination of the steering axis in the longitudinal (X–Z) plane. The deviation scenarios defined in Table 3.3 represent the combinations of upper and lower wishbone tolerances that most significantly affect camber and caster angles. By selecting the extreme cases, the analysis captures the maximum possible variation in camber and caster due to hardpoint tolerances, without having to evaluate the entire set of kinematic states.

Scenario	**Upper wishbone**	**Lower wishbone**
Max positive camber deviation	Y+ and Z-	Y- and Z+
Max negative camber deviation	Y- and Z-	Y+ and Z+
Max positive caster deviation	X- and Z-	X+ and Z+
Max negative caster deviation	X+ and Z-	X- and Z+

Table 3.3: Camber and caster tolerance deviation scenarios.

Hardpoint	Axis	T_{total} statistical $\pm$ [mm]	T_{total} worst case $\pm$ [mm]	Reference frame
U1	X	0,364	0.450	SolidWorks
	Y	0.845	1.119	
	Z	0.851	1.219	
U2	X	0.461	0.850	SolidWorks
	Y	0.845	1.119	
	Z	0.851	1.219	
U3	X	0.269	0.350	Upper wishbone
	Y	0.250	0.250	
	Z	-	-	
L1	X	0.364	0.450	SolidWorks
	Y	0.769	0.769	
	Z	0.775	0.869	
L2	X	0.461	0.850	SolidWorks
	Y	0.769	0.769	
	Z	0.851	1.219	
L3	X	0.269	0.350	Lower wishbone
	Y	0.250	0.250	
	Z	-	-	

Table 3.2: Total suspension hardpoint tolerances resulting from the tolerance chains, linearly (worst-case) and statistically, and the reference frame in which they are defined.

To plot the kinematic state of the suspension, a model is built in Python using theory from Moore [28]. Points U1, U2, L1, and L2 are defined in reference frame N, following the vehicle axes specified in ISO 8855 [29]. To define points U3 and L3, local reference systems are created that rotate around the axes through their respective interface points (U1–U2 and L1–L2). In the model, these systems are specified by three body-fixed rotations relative to reference frame N, where the rotation angles are derived from the positions of U1–U2 and L1–L2, including their tolerances. This results in 4 fixed points in space and two points U3 and L3 that can rotate around the axis through their respective interface points. To position U3 and L3, the initial angle for the local reference frame of the lower wishbone is used to fix the position of L3. Then, since the upright has a fixed length, the position of U3 can be found using the intersection of a sphere spanned by the upright around hardpoint L3 and a circle traced by U3 when rotating the upper wishbone local reference system around its axis. The complete suspension model Python code is provided in Appendix A. The kinematic model was validated through a combination of checks. First, with all tolerances set to zero, the model reproduced the nominal suspension hardpoints and corresponding static camber and caster angles. Second, several tolerance scenarios were initially verified by hand calculations and gave consistent results with the model. Lastly, intuitive changes in the geometry were tested (shifting a hardpoint in a direction where the effect on camber or caster is obvious), and the model produced the expected outcome in static variation of camber or caster. After validation, the positions of all suspension hardpoints for each deviation scenario were then used as input for the next step, where suspension travel is simulated and the camber and caster angles are plotted.

3.3.3. Simulating suspension angles

To simulate the suspension motion, DynaTune-XL Suspension Design Module [30] is used. In this program, hardpoint coordinates can be used as input to plot the resulting suspension angles during motion. Figure 3.5 illustrates the hardpoint data implemented in DynaTune-XL. Each scenario from Table 3.3 is used as input in DynaTune-XL, and the resulting suspension angles are shown in Figure 3.6. With the data from Figure 3.6, requirement R5 from Table 3.1 can be verified, the statistical variation

in camber angle stays within the ± 0.45 degrees. For the caster angle the variation stays withing ± 0.65 degrees. This indicates that tolerances may be relaxed, as the statistical variations remain within the specified limits.

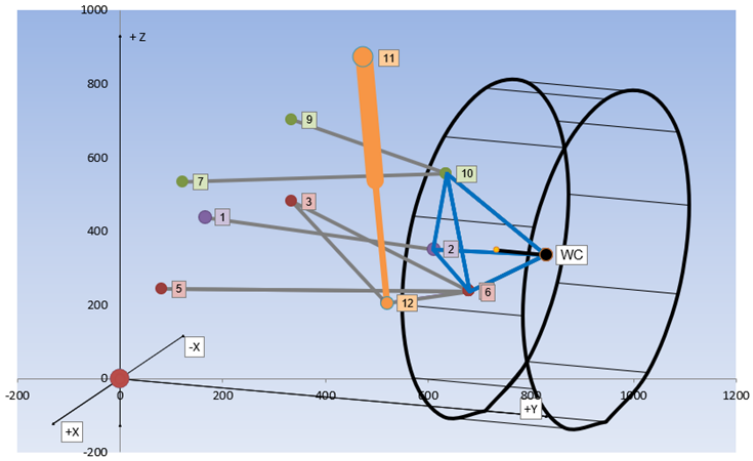

Figure 3.5: Suspension hardpoints in DynaTune-XL, including the steering link, wheel center, and the shock absorber.

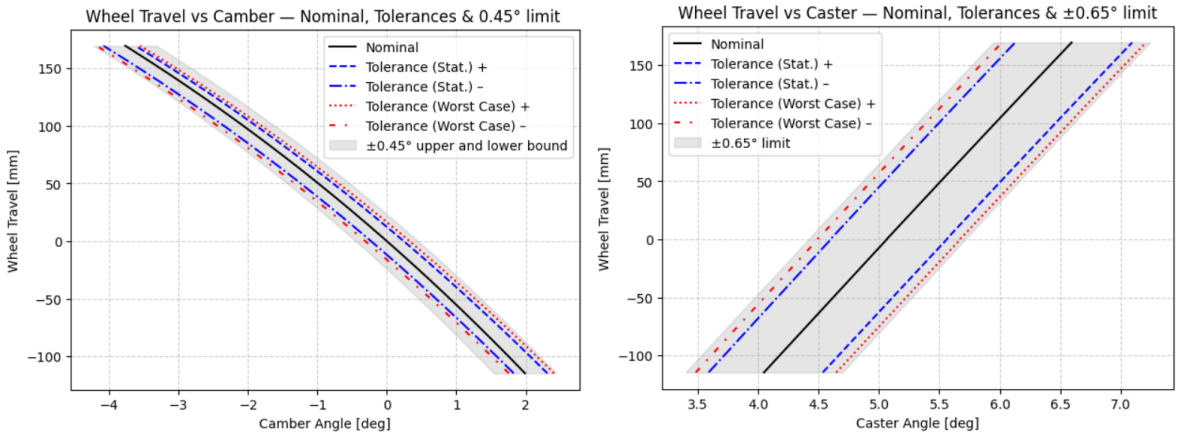

(a) Camber angle plotted against wheel travel for all tolerance deviation scenarios using statistical and linear (worst-case) tolerance chains.

(b) Caster angle plotted against wheel travel for all tolerance deviation scenarios using statistical and linear (worst-case) tolerance chains.

Figure 3.6: Nominal caster and camber angles with their min and max tolerances and their respective upper and lower bounds.

3.3.4. Tolerance relaxation

Section 3.3.3 shows that the tolerances in the prototype's double wishbone suspension can be relaxed without exceeding the specified limits. Tolerances can be broadened on the chassis or on the wishbones. Since the scope of this project is to redesign the suspension, tolerance relaxation is applied to the upper and lower wishbones. The interface between the wishbones and the chassis currently uses press-fit bearings, which require P7/J7 tolerances. Since the company specified that this bearing interface must be retained, relaxing these hardpoints is not practical since they have to be machined to a press fit. Instead, the tolerances on the suspension hardpoints U3 and L3 are relaxed. U3 and L3 connect the upper and lower wishbones to the upright with ball joints. The threaded holes on the upper and lower wishbones for the ball joints have positional tolerances of 0.5 mm. These tolerances are increased from 0.5 to 1 mm. Figure 3.7 shows that the variation in camber and caster curves stays within specified limits with the ball joint positional tolerance for both U3 and L3 increased. This tolerance relaxation can be used as input for the next step in the V-Model, the component detailed design phase.

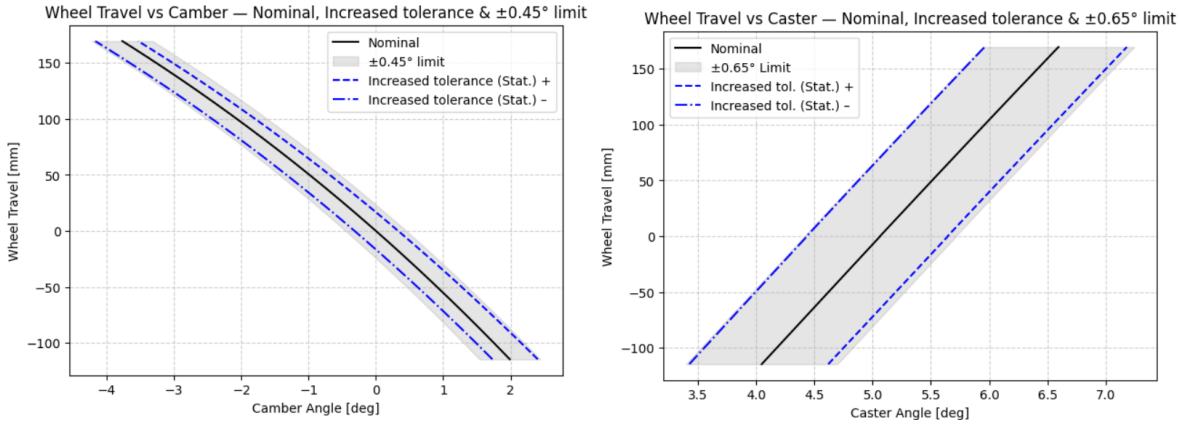

(a) Camber angle plotted against wheel travel for the nominal angle and the increased tolerance on the outer ball joints using statistical tolerance chains.

(b) Camber angle plotted against wheel travel for the nominal angle and the increased tolerance on the outer ball joints using statistical tolerance chains.

Figure 3.7: Nominal caster and camber angles with their min and max statistical variation of the increased outer ball joints tolerances.

3.4. Redesign of lower wishbone

The tolerance analysis identified that the tolerances of U3 and L3 can be relaxed. In line with the V-Model, the process now continues with the component detailed design phase. The redesign effort is focused on the lower wishbone, as it is the most complex component that experiences the highest loads, as it houses the interface with the shock absorbers. At this stage of the redesign, the question arose whether the lower wishbones should remain interchangeable between all four corners of the vehicle. In the prototype vehicle, the choice of interchangeability simplified spare parts management and increased the sample size for manufacturing; however, it required corner-specific bushings, which introduced potential issues during servicing of the suspension. The front wishbones of the prototype are also over-engineered due to higher rear-axle load cases. This redesign, therefore, focuses on a redesign specific to the front left corner of the vehicle to assess the implications of dropping the interchangeability. The front axle load case is stated as 75% of the rear axle load case based on simulation data obtained from the prototype vehicle.

In this redesign, the design for manufacturing practice is applied following approaches from the book Materials, by Michael Ashby [31], and using Ansys Granta Edupack for material and process selection. First, all the design requirements of the lower wishbone are translated into constraints and material properties to guide material and process selection, Table 3.4.

Based on the translated design requirements in Table 3.4, materials and manufacturing processes are screened in Ansys Granta Edupack. Figure 3.8 shows the initial material and process screening. Based on the manufacturing process filter in Figure 3.8 there are seven possible primary manufacturing processes that meet the requirements. A process not included in Granta Edupack is welding, since this is not primarily a shaping process; it is, however, included in the selection since it is commonly applied in suspension design to build wishbones using a welded assembly.

From the resulting selection of manufacturing processes, the following processes are excluded for practical reasons: Abrasive jet machining, grinding, and turning/boring/parting, since they are not practical as a primary shaping process for a complex 3d solid geometry, such as a lower wishbone. This leaves five potential processes: ceramic shell evaporative mold casting, sand casting, hot isostatic pressing, milling, and welding.

The current prototype uses a combination of plasma cutting, welding, and milling to shape the lower wishbones. While this method achieves very high dimensional accuracy and works well for prototype design, it is not efficient or practical during series production when producing 200 units per year. A welded tube design was also assessed but found incompatible with the existing chassis-wishbone interface, since insufficient space is available to accommodate tubes of the diameter required for the load case. Hot isostatic pressing is excluded as well, since it is a highly specialized process involving

Category	Translated design requirements
Function	Control arm for double wishbone suspension
Shape	3D solid component
Mass	Estimated range: 30–50 kg (current prototype: 38 kg)
Material family	Metals and alloys
Section thickness	Approx. 50 mm (based on current prototype)
General tolerance	$\pm$ 1 mm
Finishing tolerance	Up to J7 press fit according to ISO standards [32, 33]
Batch size	200 units/year
Yield strength	500–700 MPa (based on current material: 700 MPa, using 0.75 × existing use case)
Tensile strength	600–900 MPa (based on current material: 850–1000 MPa, using 0.75 × existing use case)
Impact toughness	Minimum 27 J absorbed in Charpy V-notch test at $-46\,^{\circ}\mathrm{C}$

Table 3.4: Translated design requirements for the suspension lower wishbone following Ashby's design-led approach.

complex equipment and powder metal as base material. This leaves two casting processes: Sand casting and ceramic shell evaporative mold casting. Both processes require finishing by machining at the bearing contact surfaces to meet the design requirements. Ceramic shell evaporative mold casting can achieve better tolerances and surface finish than sand casting [34]. However, machining is still required at the contact surfaces, making the advantage of ceramic shell evaporative mold casting diminish. Therefore, sand casting is selected as the most suitable primary shaping process.

Based on this process, an advanced material search is done to select materials that meet all the design requirements and are compatible with casting (Figure 3.8). The results of this search are shown in Figure 3.9, and a detailed list of all materials is provided in Appendix B. An important requirement for material selection is R6 from Table 3.1, which specifies a Charpy V-notch impact test at $-46,^{\circ}\mathrm{C}$. The materials databases in Granta Edupack provide only minimal service temperature and fracture toughness values, which can serve as indicators but do not fully verify compliance with this requirement.

With a suitable manufacturing process and a selection of materials, the redesign can begin. Since the interchangeability is abandoned, the redesign is made specific to the front left corner of the vehicle, focusing on a new wishbone–shock absorber interface and a reduced load case. The package space constraints of the current prototype vehicle are maintained in the redesign. During the redesign, key casting considerations are taken into account, including uniform section thickness and round radii, to minimize casting defects. Additionally, mold design is considered, with a focus on avoiding negative draft angles and facilitating production with a simple two-part mold. Further verification of the redesign in Section 3.5 will narrow down the material selection.

The design is made using SolidWorks. Figure 3.10 shows the redesigned wishbone; green surfaces indicate surfaces that need to be machined after casting. The interfaces with the shock absorbers and outer ball joint are shown in Figure 3.11. The three triangular cutouts serve to make the material section thickness more uniform, preventing defects during casting caused by differences in cooling rate due to the non-uniform section thickness. The original design of the prototype lower wishbone is added in Appendix F for reference. Figure 3.12 shows a two-piece mold design for the redesigned lower wishbone. The redesign allows for the part to be cast using a two-part mold.

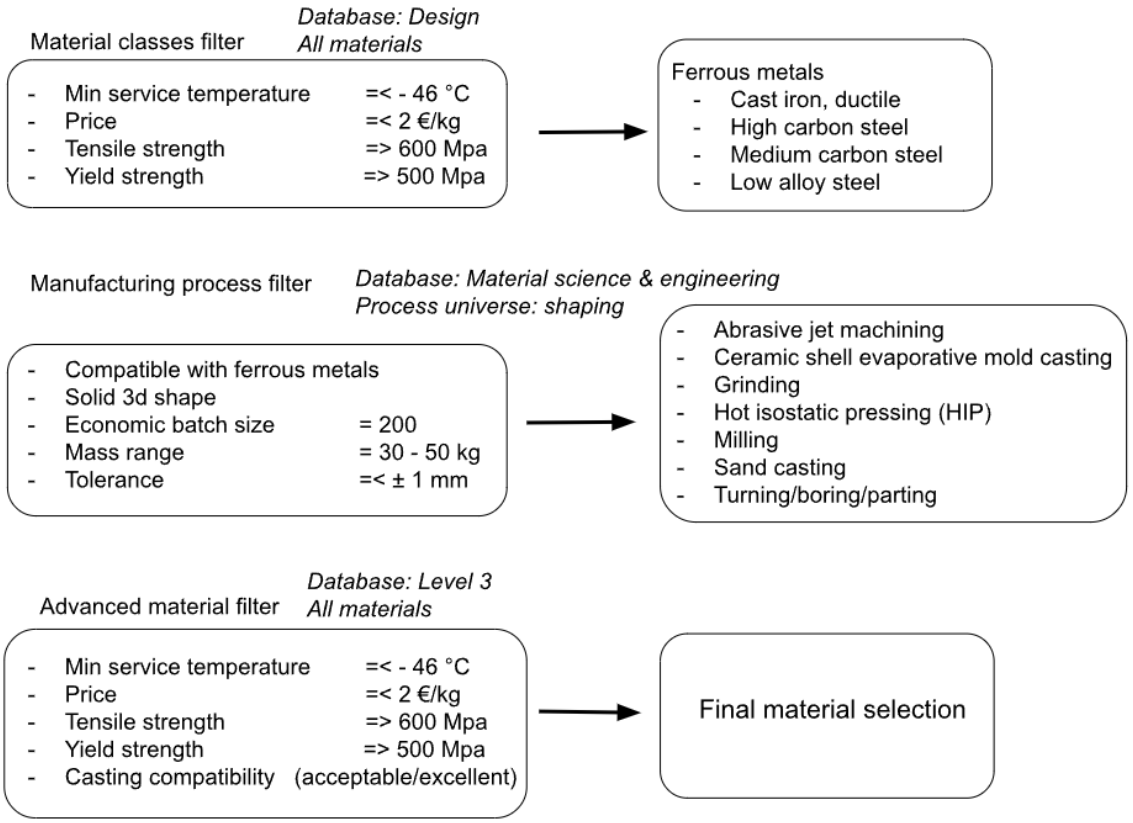

Figure 3.8: Material and process selection used in Ansys Granta Edupack 2024.

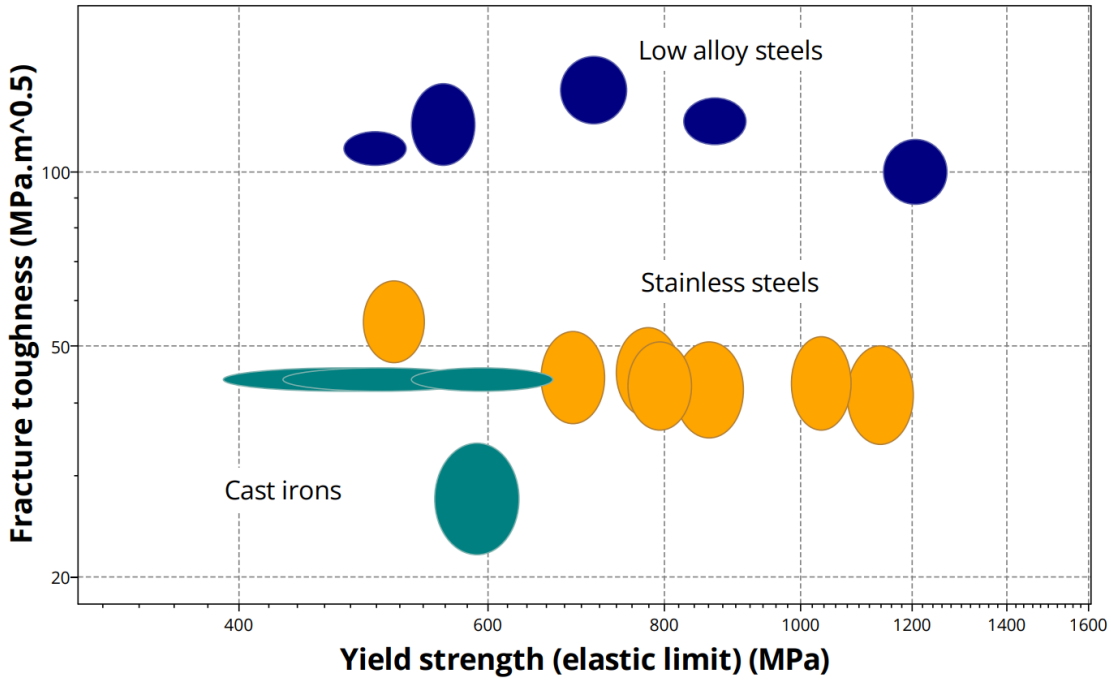

Figure 3.9: Final material selection in Ansys Granta Edupack, yield strength vs fracture toughness. Low alloy steels in blue, stainless steels in orange, and cast irons in teal.

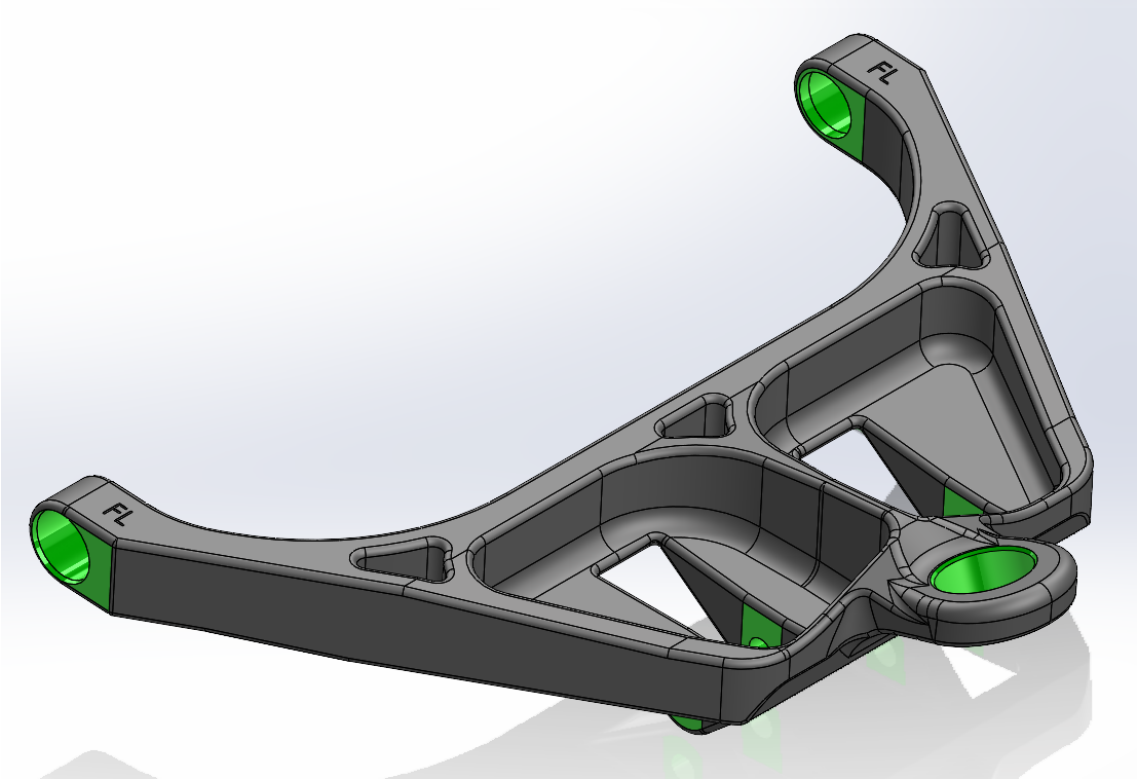

Figure 3.10: CAD model of the redesigned lower wishbone in SolidWorks, all surfaces that need to be machined after casting are marked in green.

3.5. Structural verification of redesigned lower wishbone

To determine whether the redesigned lower wishbone can meet requirement R2 (Table 3.1), a structural analysis is done using Altair SimSolid corresponding with the component verification phase on the right side of the V-Model. Predefined load cases for a drop test, step test, and curb strike, as illustrated in Figure 3.13, are used to do the structural analysis. For the step test, a forward and rearward scenario is defined, for the curb strike inside wheel and outside wheel is defined.

In this analysis, inertia relief is applied. Inertia relief is a numerical method for analyzing unconstrained structures: instead of imposing artificial supports, the method introduces inertial accelerations that balance the applied loads, placing the part in static equilibrium. Any imbalance in the loads is reacted to by the inertia forces, making it possible to run the analysis without constraints. This allows for the evaluation of the lower wishbone in isolation. All loads are specified at the ball joint centers. For the ball joint at L3, a preload of 975 Nm is applied on the M74x1.5 bolt. On the interface points with the shock absorber, a preload of 200 Nm is applied on the M24x1.5 bolts.

Material properties from a selection of materials (Table 3.5) from section 3.4 are exported from Granta Edupack. Edupack uses a range for some material properties like yield strength and ultimate tensile strength; in these cases, the median value of the range is used for the structural analysis. For each load case, a maximum and an extreme load case are defined. These load cases already include a safety factor; this allows the material to be stressed up to its yield point in this analysis. For the maximum load case, no plastic deformation is allowed. For the extreme load case, plastic deformation is allowed, but no fracture.

In this analysis, the safety factor is defined as the ratio of the material yield strength to the maximum von Mises stress obtained from the simulation in SimSolid. A safety factor greater than or equal to 1 indicates elastic behavior, while a value below 1 signifies plastic deformation. All materials from Table 3.5 are included in the structural analysis and the results are shown in Appendix D. For the cast iron materials, plastic deformations occurred at the maximum drop test load case. For the low alloy steels, the results are shown in Figure 3.15. Figure 3.14 shows the stress concentrations in the lower wishbone of SAE 4130 low alloy steel for the extreme drop test load case. Stress concentrations arise at the neck of the outer ball joint interface, resulting in plastic deformation and a minimum safety factor of 0.92.

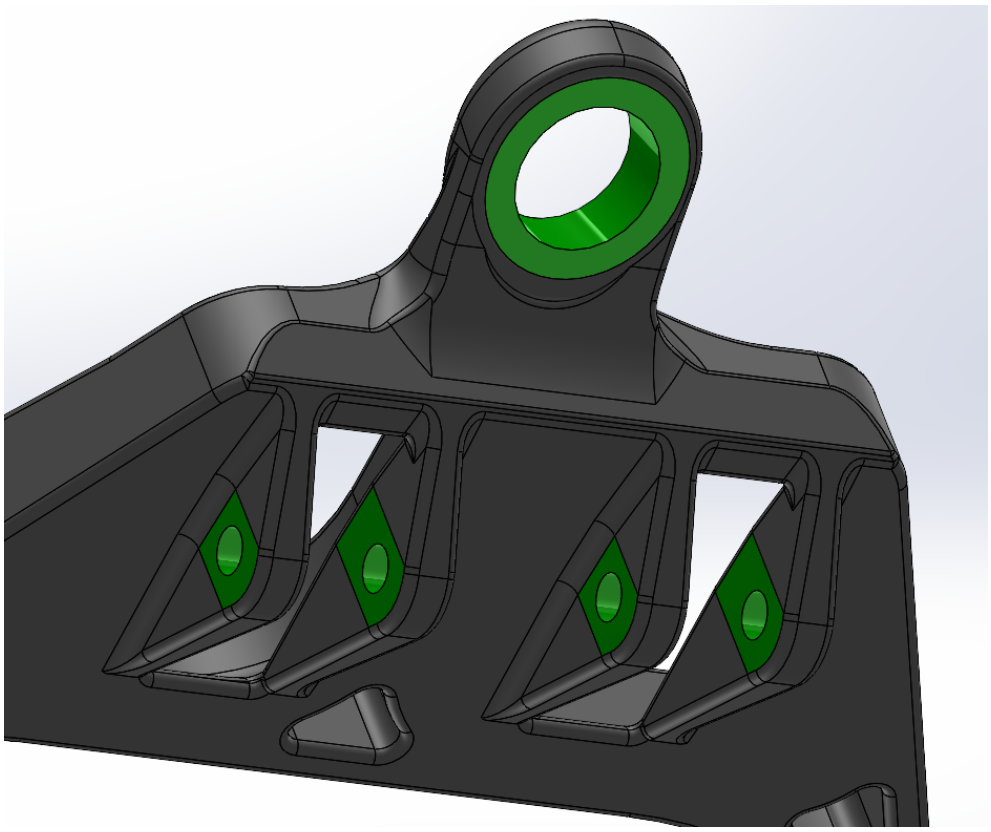

Figure 3.11: CAD model of the redesigned lower wishbone in SolidWorks, zoomed in on the interfaces for the shock absorbers and the outer ball joint interface.

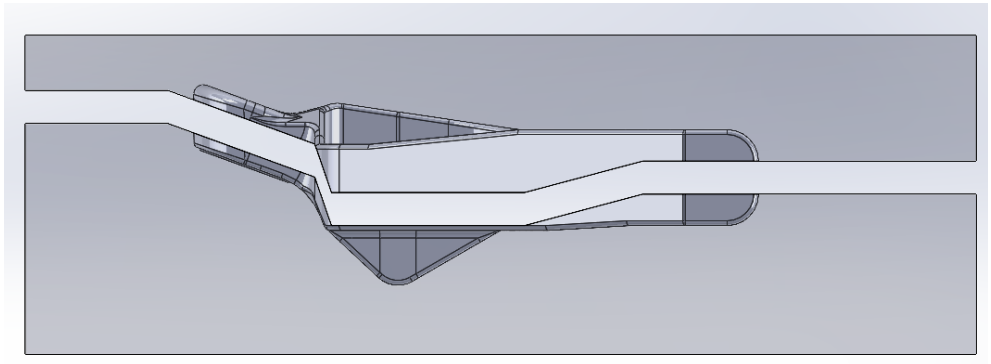

Figure 3.12: Mold design for the redesigned lower wishbone, the mold is made from 2 parts with no negative draft angles.

Material category (casting compatibility)	**Material grade**
Cast irons (acceptable)	Pearlitic malleable, EN GJMB 600-3, BS EN 1562
	Pearlitic malleable, EN GJMB 650-2, BS EN 1562
	Pearlitic malleable, EN GJMB 700-2, BS EN 1562
Low alloy steels (excellent)	SAE 4130, cast, quenched & tempered
	SAE 8630, cast, quenched & tempered
	SAE 4335M, cast, quenched & tempered

Table 3.5: Candidate materials for structural analysis.

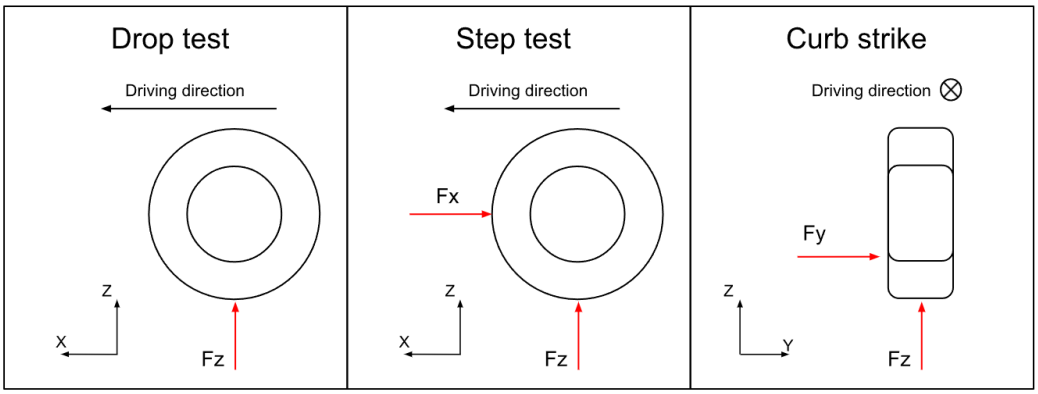

Figure 3.13: Load case definition for the drop test, step test, and curb strike.

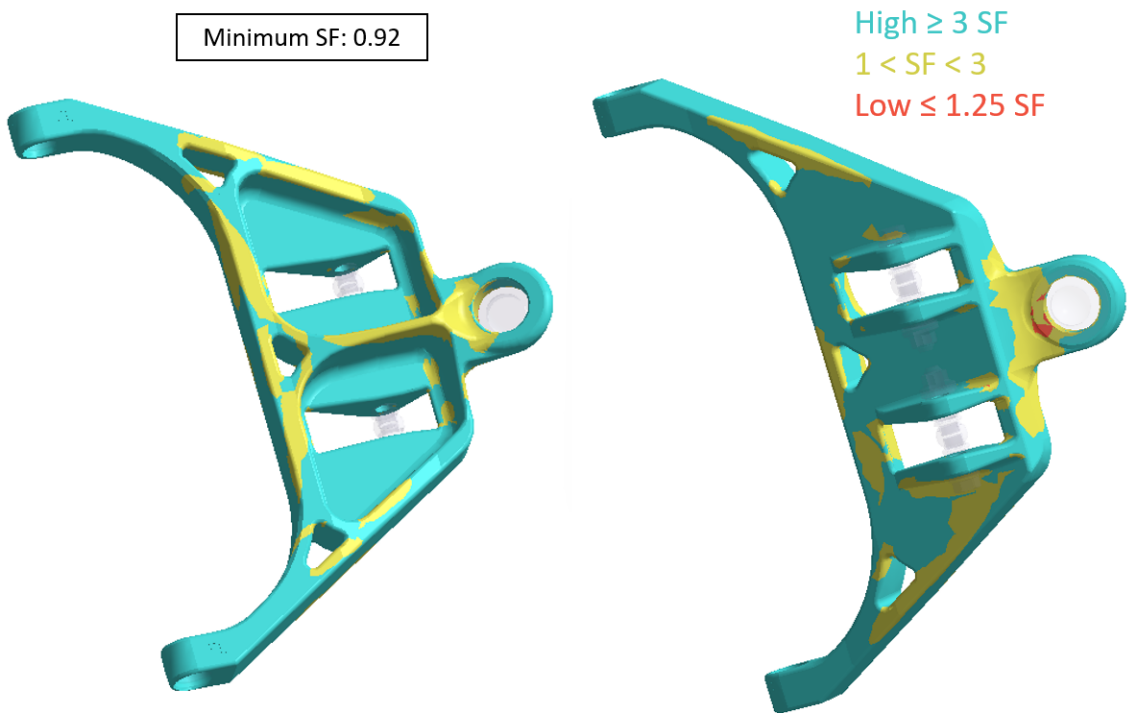

Figure 3.14: Structural analysis of the lower wishbone redesign using SAE 4130 low alloy steel and the extreme drop test load case.

		Front axle load		
Material	**Low alloy steel**	**SAE 4130**	**SAE 8630**	**SAE 4335 M**
		Safety factor		
Maximum	Drop test	1,01	1,23	1,76
	Step test FWD	1,51	1,85	2,63
	Step test RWD	1,26	1,53	2,18
	Curb strike test IW	1,78	2,17	3,1
	Curb strike test OW	1,74	2,13	3,03
Extreme	Drop test	0,92	1.13	1.61
	Step test FWD	1,23	1,5	2,13
	Step test RWD	1,09	1,33	1,89

Figure 3.15: Minimum safety factors for all load cases across various materials.

The structural analysis demonstrates that all three low alloy steels considered (SAE 4130, SAE 8630, and SAE 4335M) satisfy the predefined load case requirements. For the maximum load cases, the safety factors remained above 1, meaning no plastic deformation occurred. Under the extreme load case with SAE 4130, localized plastic deformation is observed, but the maximum von Mises stress remained well below the ultimate tensile strength, indicating that only plastic deformation occurred and no fracture.

4

Discussion

4.1. Evaluation of V-model approach

The Systems Engineering V-Model proved especially valuable in this project by providing a structured design process, improving requirement definition, and reducing risk. First, the structured design process helped maintain a clear overview of the suspension redesign within the wider vehicle system. By breaking the system down into subsystems and components, the method ensured that the lower wishbone was not redesigned in isolation, but linked back to system-level requirements. Second, the V-Model strengthened requirement definition while at the same time reducing risk. The V-Model requires that each requirement be linked to a verification or validation step; wrongly formulated requirements are therefore identified early in the process. This made requirements more concrete and verifiable while reducing the chance of discovering problems later on. For example, requirement R5 was explicitly tied to the tolerance analysis, which reduced the risk of over-engineering by showing where tolerances could be safely relaxed. Similarly, the verification of the wishbone redesign through structural analysis reduced the risk that a manufacturable design would later fail to meet strength requirements. The V-Model approach does require significant upfront investment in defining stakeholder needs and requirements. For smaller projects, this may appear time-consuming and cumbersome, and it is not necessarily faster in the early phases. However, by preventing costly redesigns and ensuring requirements are verifiable from the start, it can save considerable time and effort later in the project. An important observation is that the V-Model is not a rigid sequence. This was demonstrated when the bearing interface constraint was introduced after architecture selection, necessitating a step back to system-level requirements without compromising traceability.

An additional observation, although not directly part of this project, is that the V-Model also makes the risks of skipping steps explicit. This highlights a broader strength of the method in maintaining accountability when development conditions are constrained.

4.2. Tolerance and kinematic analysis

The tolerance analysis showed how dimensional variation in the chassis, chassis wishbone interfaces, and wishbones propagates into camber and caster angles during wheel travel. A key insight is that the current prototype suspension tolerances were stricter than necessary. The analysis demonstrated that tolerances on the upper and lower wishbone could be relaxed while still keeping camber and caster variation within predefined limits. However, it should be noted that tolerances of the upright and the wheel assembly were not included; their impact is expected to be minor, contributing only about $\pm 0.01^\circ$ to the total variation in camber.

Only a specific set of worst-case scenarios for the camber and caster angle was considered. This is a conservative method that yields safe margins but does not accurately reflect the likelihood of these variations in reality. A Monte Carlo approach would give a more realistic distribution of tolerances and could be used to assess the most probable suspension behavior.

The assumption of rigid suspension components and ideal ball joints may underestimate real-world variation in suspension angles.

Since the scope of this project was to redesign the suspension, the tolerance relaxation was applied to the wishbones. Another option would be to apply this relaxation to the chassis. The expectation is that loosening tolerances on the chassis would lead to greater variation in suspension angles, mainly because the chassis defines the rotation axes of the upper and lower wishbones. Further research could indicate if this is indeed the case.

4.3. Redesign constraints and material selection

A key design constraint was the mandated retention of the chassis press-fit bearing interface introduced after the selection of the double wishbone suspension. This constraint limited the ability to explore welded wishbone concepts or chassis-side tolerance relaxation on the wishbones. While the current redesign optimized manufacturability via sand casting, broader design freedom is expected to result in an even simpler, lower wishbone redesign if alternative chassis wishbone interfaces were considered. Regarding material selection, the use of Granta Edupack provided an efficient way to screen and compare materials for the redesigned lower wishbone. However, reliance on the database also represents a potential blind spot, as materials not included in Edupack were not considered in the selection process. While database values indicate that the candidate materials for the redesigned lower wishbone may meet the low-temperature toughness requirement (R6), this has not been experimentally verified within the scope of this project. Full compliance with R6, therefore, requires Charpy V-notch testing at $-46,^{\circ}\,\mathrm{C}$ on material samples, which is recommended as part of further verification. Material supply chain availability also warrants further investigation before series production. The redesign was only verified virtually and not experimentally. As such, fatigue behavior and environmental effects remain untested and could alter the final geometry and material of the redesign.

4.4. Interchangeability of lower wishbones

In the prototype suspension, the lower wishbones were designed to be interchangeable across all four corners of the vehicle. This approach offers benefits when it comes to the supply chain management of spare parts. It also increases the manufacturing sample size, a benefit which is not fully utilized in the current prototype. The interchangeability design also introduced some drawbacks. In the redesign, interchangeability was dropped in favor of optimization. The design was made specifically for the front left corner of the vehicle. This allowed for more freedom in the redesign and resulted in a different manufacturing technique and a simplified wishbone shock absorber interface. To make an informed decision on whether interchangeability should be retained, a full lifecycle cost-benefit analysis of both options should be conducted.

4.5. Structural analysis

For the structural analysis of the lower wishbone, Altair SimSolid was used to rapidly evaluate multiple load cases and materials. The meshless solver allows for quick comparison of different materials and designs, making it well-suited for the early stages of the V-model where multiple concepts must be screened against user requirements. However, SimSolid is not intended to replace traditional finite element analysis in all applications. While it provides reliable global stiffness and strength trends, localized stress concentrations and certification-critical results are best validated with a mesh-based FEA approach. Therefore, for the final detailed design phase of the V-Model, a conventional FEA tool with explicit meshing is recommended to verify the results obtained in SimSolid. In line with the right leg of the V-Model, verification and validation should also include fatigue life simulation and testing, quarter-vehicle suspension tests, and full-vehicle testing to confirm the load cases.

5

Conclusion

This work demonstrated the application of the Systems Engineering V-model to the redesign of a military terrain vehicle suspension. By following a requirement-based and verification-driven approach, traceability from stakeholder needs to system-level requirements and component verification is ensured.

The key outcomes can be summarized as follows: First, the double wishbone suspension architecture was identified as the most suitable solution for the new vehicle platform, meeting requirements on chassis compatibility, vehicle mass, dimensional constraints, and mobility.
Second, a tolerance analysis method was established linking component-level dimensional tolerances to variations in suspension angles. This method demonstrated that the current prototype suspension had room for tolerance relaxation, given the allowable variation in camber and caster angles. The positional tolerance of the outer ball joints of the lower and upper wishbones can be increased from 0.5 to 1 mm while still meeting the requirements.
Based on these insights, a redesign is made focusing on manufacturability and optimizing the design for the front left corner of the vehicle. The prototype used a combination of plasma cutting, welding, and milling to shape the lower wishbone and required corner-specific bushings to ensure interchangeability. The redesign is tailored for the front left corner of the vehicle, uses relaxed tolerances at the outer ball joint, and eliminates the need for bushings by allowing direct mounting of the shock absorbers. The redesign also switches to a combination of sand casting and finishing milling, which simplifies manufacturing and is better suited for series production.
Structural verification through simulation showed that the redesign using multiple material options can withstand the required load cases.

A case study is presented on the application of the V-Model within the automotive/defense sector. This case study demonstrates that the V-model, traditionally used in aerospace and software development, offers three main benefits for suspension system development in the automotive industry: A structured, traceable design process, clear, verifiable requirements, and reduced risk by linking each requirement on the left side of the V-Model to a verification step on the right side. This project also shows that the V-Model is not a strict sequence; its flexibility allows stepping back up the left leg to earlier system-level requirements, which is often useful in the early stages of design.
A tolerance analysis method is presented that relates suspension component tolerances to variations in suspension angle, providing designers with a practical tool to evaluate the impact of tolerances on suspension behavior. This method can be used to determine hardpoint tolerances based on predefined limits in variation of suspension angles or to determine the variation of suspension angles based on existing hardpoint tolerances. Finally, the redesign of the lower wishbone is presented, providing a solid foundation for transitioning from prototype to series production.

References

[1] Shakeel N. Avadhany et al. “Regenerative, semi-active shock absorber technology “GenShock®” for improved ride handling and fuel economy on combat and tactical vehicles”. In: *Proceedings of the Ground Vehicle Systems Engineering and Technology Symposium*. National Defense Industrial Association, Aug. 2010. DOI: 10.4271/2024-01-3176.

[2] R. J. Hayes et al. “Design and Testing of an Active Suspension System for a 2-1/2 Ton Military Truck”. In: SAE International, Apr. 2005. DOI: 10.4271/2005-01-1715.

[3] Andrea C. Wray et al. “Magneto-Rheological Fluid Semiactive Suspension System Performance Testing on a Stryker Vehicle”. In: SAE International, Apr. 2006. DOI: 10.4271/2006-01-1379.

[4] Leo Davis. “Simulation and test of HMMWV with active controls”. In: *Proceedings of SPIE - The International Society for Optical Engineering*. Vol. 5805. Type: Conference paper. 2005, pp. 41–53. DOI: 10.1117/12.609730. URL: https://www.scopus.com/inward/record.uri?eid=2-s2.0-27544447923&doi=10.1117%2f12.609730&partnerID=40&md5=81f46dce2f43e058295c78acdd4e885b.

[5] Francis B. Hoogterp. “Active suspension technology for combat vehicles”. In: *Proceedings of SPIE - The International Society for Optical Engineering*. Vol. 10281. Type: Conference paper. 1995, pp. 25–48. DOI: 10.1117/12.205543. URL: https://www.scopus.com/inward/record.uri?eid=2-s2.0-0029484043&doi=10.1117%2f12.205543&partnerID=40&md5=28dce4f9d98b1aacf5984678556eafe8.

[6] D.A. Crolla, G.R. Firth, and D.N.L. Horton. “Independent vs. Axle Suspension for On/Off Road Vehicles”. In: SAE International, Sept. 1992. DOI: 10.4271/921662.

[7] Y. Gene Liao, Molly O’Malley, and Allen M. Quail. “Experimental and numerical analysis of the dynamic behavior of variant suspensions for tactical trucks”. In: *Proceedings of the Institution of Mechanical Engineers, Part D: Journal of Automobile Engineering* 228.6 (2014). Type: Article, pp. 674–688. DOI: 10.1177/0954407013498863. URL: https://www.scopus.com/inward/record.uri?eid=2-s2.0-84899121300&doi=10.1177%2f0954407013498863&partnerID=40&md5=fb94bd1bb67b29e0b398c1cf489096e8.

[8] Günter Hohl. “Off-Road Vehicles (Wheeled and Tracked)”. en. In: *Road and Off-Road Vehicle System Dynamics Handbook*. Ed. by Manfred Ploechl. CRC Press, Oct. 2013, pp. 395–476. ISBN: 9780849333224/9781420004908. DOI: 10.1201/b15560-15. URL: http://www.crcnetbase.com/doi/abs/10.1201/b15560-15.

[9] Günter H Hohl and Alexander Corrieri. “Basic Considerations for the Concepts of Wheeled off-Road Vehicles”. en. In: *Society of Automotive Engineers of Korea* (June 2000).

[10] Wendell Tackett, Jeffrey Lovell, and Chris Brown. “ADDRESSING THE CHALLENGES OF PROVIDING MOBILITY AND MANEUVERABILITY FOR TACTICAL WHEELED VEHICLES”. In: National Defense Industrial Association, Aug. 2016. DOI: 10.4271/2024-01-3603.

[11] John LaPlante. “Upgraded suspension systems improve mobility and survivability of ground vehicles”. In: *Proceedings of the Ground Vehicle Systems Engineering and Technology Symposium*. National Defense Industrial Association, Aug. 2011. DOI: 10.4271/2024-01-3270.

[12] Joseph Beno et al. “ROAD BREAKAWAY ROLLOVER MITIGATION WITH HIGH PERFORMANCE ELECTROMECHANICAL ACTIVE SUSPENSION SYSTEMS”. In: National Defense Industrial Association, Aug. 2015. DOI: 10.4271/2024-01-3538.

[13] David E Kline. “Geometric Design of Independent Suspension Linkages”. en. In: *University of Michigan* (2018). URL: https://hdl.handle.net/2027.42/147506.

[14] James Balkwill. “Chapter 7 - Suspension Kinematics”. In: *Performance Vehicle Dynamics*. Butterworth-Heinemann, Jan. 2018, pp. 197–239. ISBN: 978-0-12-812693-6. DOI: 10.1016/B978-0-12-812693-6.00007-9. URL: https://www.sciencedirect.com/science/article/pii/B9780128126936000079.

[15] Francesco Bucchi and Basilio Lenzo. “Analytical Derivation and Analysis of Vertical and Lateral Installation Ratios for Swing Axle, McPherson and Double Wishbone Suspension Architectures”. en. In: *Actuators* 11.8 (Aug. 2022), p. 229. ISSN: 2076-0825. DOI: 10.3390/act11080229. URL: https://www.mdpi.com/2076-0825/11/8/229.

[16] Y. Gene Liao, Brandon Card, and John Wasylyk. “COMPARATIVE ANALYSIS OF VIRTUAL AND EXPERIMENTAL PROVING GROUND FOR MEDIUM-DUTY TACTICAL TRUCK USING VARIETY OF SUSPENSIONS”. In: National Defense Industrial Association, Aug. 2016. DOI: 10.4271/2024-01-3618.

[17] Mohamed Mostafa Khalil, Mostafa R.A. Atia, and Mohamed H. Mabrouk. “Improving Vehicle Rollover Resistance Using Fuzzy PID Controller of Active Anti-Roll Bar System”. In: *SAE International Journal of Passenger Cars - Mechanical Systems* 12.1 (Dec. 2018). Publisher: SAE International, pp. 35–50. DOI: 10.4271/06-12-01-0003.

[18] Glenn R. Wendel, Joe Steiber, and Gary L. Stecklein. “Regenerative active suspension on rough terrain vehicles”. In: *SAE Technical Papers*. Type: Conference paper. 1994. DOI: 10.4271/940984. URL: https://www.scopus.com/inward/record.uri?eid=2-s2.0-85072440913&doi=10.4271%2f940984&partnerID=40&md5=6e0c3fbf755796c26830ec66262e52df.

[19] J. H. Beno et al. “Experimental Comparison of Losses for Conventional Passive and Energy Efficient Active Suspension Systems”. In: SAE International, Mar. 2002. DOI: 10.4271/2002-01-0282.

[20] Markus Maurer. “Automotive Systems Engineering: A Personal Perspective”. In: *Automotive Systems Engineering*. Ed. by Markus Maurer and Hermann Winner. Berlin, Heidelberg: Springer Berlin Heidelberg, 2013, pp. 17–35. ISBN: 978-3-642-36455-6. DOI: 10.1007/978-3-642-36455-6_2. URL: https://doi.org/10.1007/978-3-642-36455-6_2.

[21] M Azizuddin Imtiaz. *Unlocking the V-Model: A Beginner’s Guide to Systems Engineering*. 2024. URL: https://www.linkedin.com/pulse/unlocking-v-model-beginners-guide-systems-engineering-imtiaz-nkkyc.

[22] Andrew John Prusinowski. “Exploring the Effect of Manufacturing Tolerances on the Front Suspension Performance of a Formula SAE Vehicle Relative to Design Targets”. English. In: SAE International, Dec. 2008. DOI: 10.4271/2008-01-2952. URL: https://saemobilus-sae-org.tudelft.idm.oclc.org/papers/exploring-effect-manufacturing-tolerances-front-suspension-performance-a-formula-sae-vehicle-relative-design-targets-2008-01-2952.

[23] Roberto Rotundo and Lorenzo Amato. “Robust Design Of An Automotive Suspension: A Study On The Reduction Of Tolerances”. English. In: SAE International, Apr. 2008. DOI: 10.4271/2008-01-0712. URL: https://saemobilus.sae.org/papers/robust-design-automotive-suspension-a-study-reduction-tolerances-2008-01-0712.

[24] Matteo Lanzavecchia et al. “Road Vehicle Robust Design: Chassis and Suspension Tolerances Impact on the Handling and Stability Behaviour”. English. In: SAE International, Apr. 2008. DOI: 10.4271/2008-01-0710. URL: https://saemobilus.sae.org/papers/road-vehicle-robust-design-chassis-suspension-tolerances-impact-handling-stability-behaviour-2008-01-0710.

[25] S. K. Kim et al. “Accumulated tolerance analysis of suspension by geometric tolerances based on multibody elasto-kinematic analysis”. en. In: *International Journal of Automotive Technology* 17.2 (Apr. 2016). Company: Springer Distributor: Springer Institution: Springer Label: Springer Number: 2 Publisher: The Korean Society of Automotive Engineers, pp. 255–263. ISSN: 1976-3832. DOI: 10.1007/s12239-016-0025-x. URL: https://link-springer-com.tudelft.idm.oclc.org/article/10.1007/s12239-016-0025-x.

[26] Vladislav Borisenko et al. “K&C suspension parameters stability by production tolerances”. en. In: *E3S Web of Conferences* 140 (2019). Publisher: EDP Sciences, p. 07007. ISSN: 2267-1242. DOI: 10.1051/e3sconf/201914007007. URL: https://www.e3s-conferences.org/articles/e3sconf/abs/2019/66/e3sconf_eece18_07007/e3sconf_eece18_07007.html.

[27] Fritz Scholz. *Tolerance Stack Analysis Methods*. Research and Technology Report. December 1995. Boeing Information & Support Services, Dec. 1995.

[28] Jason K. Moore. *Learn Multibody Dynamics*. Aug. 2022. URL: https://moorepants.github.io/learn-multibody-dynamics/.

[29] International Organization for Standardization. *ISO 8855:2011 Road vehicles – Vehicle dynamics and road-holding ability – Vocabulary*. Standard. ISO 8855:2011(E). Geneva, Switzerland, 2011.

[30] DynaTune-XL. *DynaTune-XL Suspension Design Module*. https://www.dynatune-xl.com/dynatune-sdm.html. 2025.

[31] Michael F. Ashby, Hugh Shercliff, and David Cebon. *Materials: Engineering, Science, Processing and Design*. 4th ed. Elsevier Butterworth-Heinemann, 2019. ISBN: 9780081023761.

[32] *Geometrical product specifications (GPS) — ISO code system for tolerances on linear sizes — Part 1: Basis of tolerances, deviations and fits*. Geneva, Switzerland: International Organization for Standardization, 2010.

[33] *Geometrical product specifications (GPS) — ISO code system for tolerances on linear sizes — Part 2: Tables of standard tolerance classes and limit deviations for holes and shafts*. Geneva, Switzerland: International Organization for Standardization, 2010.

[34] *Ansys® Granta EduPack*. Release 2024 R1. Materials education and selection software. ANSYS, Inc., 2024.

A

Python kinematic model

```
"""
import sympy as sm
import sympy.physics.mechanics as me
import matplotlib.pyplot as plt
from mpl_toolkits.mplot3d import Axes3D
import numpy as np

# symbols
q1, q2, q3, q4, q5, q6, U1X, U1Y, U1Z, U2X, U2Y, U2Z, U3X, U3Y, U3Z, L1X, L1Y, L1Z, L2X, L2Y, L2Z, L3X, L3Y, L3Z, Upright_L = sm.symbols(
    "q1, q2, q3, q4, q5, q6, U1X, U1Y, U1Z, U2X, U2Y, U2Z, U3X, U3Y, U3Z, L1X, L1Y, L1Z, L2X, L2Y, L2Z, L3X, L3Y, L3Z, Upright_L"
)

# Define reference frames
N = me.ReferenceFrame('N') #Global reference frame according to ISO 8855
U = me.ReferenceFrame('U') #Upper control arm reference frame
L = me.ReferenceFrame('L') #Lower control arm reference frame
S = me.ReferenceFrame('S') #Solid works reference frame
A = me.ReferenceFrame('A') #Intermediate reference frame to calculate q2
B = me.ReferenceFrame('B') #Intermediate reference frame to calculate q5

N.orient_body_fixed(S, (-sm.pi/2, -sm.pi/2, 0), 'XZY')

# Points
O = me.Point('O') #ISO 8855 origin
D = me.Point('D') #Dynatune origin
WC = me.Point('WC') # wheel center
SU = me.Point('SU') # shock upper center
SL = me.Point('SL') # shock lower center
TI = me.Point('TI') #Steering link chassis hardpoint
TO = me.Point('TO') #Steering link wheel hardpoint

U1, U2, U3 = me.Point('U1'), me.Point('U2'), me.Point('U3')
L1, L2, L3 = me.Point('L1'), me.Point('L2'), me.Point('L3')
U3U, L3L = me.Point('U3U'), me.Point('L3L') # Used to calculate scalar values for U3_new and L3_new
U3_new, L3_new = me.Point('U3_new'), me.Point('L3_new')

# Assign numerical values to coordinates, imported from wireframe sketch solidworks front left wheel
U1X = ;  U1Y = ; U1Z =
U2X = ;  U2Y = ; U2Z =
U3X = ;  U3Y = ; U3Z =
L1X = ;  L1Y = ; L1Z =
L2X = ;  L2Y = ; L2Z =
L3X = ;  L3Y = ; L3Z =

# Set tolerances for all hardpoints in xyz directions in Solidworks reference frame, values are collected from excel tol. sheets
# Make sure tolerances xyz are in solidworks reference frame.
U1X_t = 0; U1Y_t = -0.844902953; U1Z_t = -0.850800212
U2X_t = 0.4; U2Y_t = -0.844902953; U2Z_t = -0.850800212
L1X_t = 0.4; L1Y_t = 0.769; L1Z_t = 0.775474693
L2X_t = 0; L2Y_t = 0.769; L2Z_t = 0.850800212

# use local reference frames for the U3 and L3 tolerances
U3X_t = -0.509901951; U3Y_t = 0; U3Z_t = 0
```

```
L3X_t = 0.509901951; L3Y_t = 0; L3Z_t = 0



# position variables to set coordinates
U1X_pos = U1X + U1X_t; U1Y_pos = U1Y + U1Y_t; U1Z_pos = U1Z + U1Z_t
U2X_pos = U2X + U2X_t; U2Y_pos = U2Y + U2Y_t; U2Z_pos = U2Z + U2Z_t
L1X_pos = L1X + L1X_t; L1Y_pos = L1Y + L1Y_t; L1Z_pos = L1Z + L1Z_t
L2X_pos = L2X + L2X_t; L2Y_pos = L2Y + L2Y_t; L2Z_pos = L2Z + L2Z_t

# Set positions

D.set_pos(O, -467.18 * N.z)
WC.set_pos(O, 882.76 * S.x + 0.49 * S.z)
SU.set_pos(O, 505 * S.x + 521.24 * S.y -2.04 * S.z)
SL.set_pos(O, 551.84 * S.x -181.77 * S.y + -2.04 * S.z)
TI.set_pos(O, 250.01 * S.x + 100 * S.y + 205 * S.z)
TO.set_pos(O, 716.57 * S.x + 58.87 * S.y + 184.99 * S.z)

U1.set_pos(O, U1X_pos * S.x + U1Y_pos * S.y + U1Z_pos * S.z)
U2.set_pos(O, U2X_pos * S.x + U2Y_pos * S.y + U2Z_pos * S.z)
U3.set_pos(O, U3X*S.x + U3Y*S.y + U3Z*S.z) # U3 tolerances are added later in the code to the
     U3_new point.
L1.set_pos(O, L1X_pos * S.x + L1Y_pos * S.y + L1Z_pos * S.z)
L2.set_pos(O, L2X_pos * S.x + L2Y_pos * S.y + L2Z_pos * S.z)
L3.set_pos(O, L3X*S.x + L3Y*S.y + L3Z*S.z) # L3 tolerances are added later in the code to the
     L3_new point.

r_U1_U2 = U2.pos_from(U1)
r_U1_U3 = U3.pos_from(U1)
r_L1_L2 = L2.pos_from(L1)
r_L1_L3 = L3.pos_from(L1)
r_L3_U3 = U3.pos_from(L3)

r_U1_U2_N =r_U1_U2.express(N)
r_L1_L2_N =r_L1_L2.express(N)

print('q2,q4,q5 should be zero when all tolerances are zero. Angles are defined using the
    right-hand rule')
print('Check that the tolerances are translated to their correct axis, excel tol sheets are
    in ISO 8855 axis')

# q1 angle between U1 and U2 around the Y axis (ISO 8855), check q1 sign convention with
    right-hand rule
q1 = -sm.atan2(r_U1_U2_N.dot(N.z), r_U1_U2_N.dot(N.x))
print('q1 =',q1)

# q2 angle between r_U1_U2 and the new x-axis around the Z- axis (ISO 8855)
# First rotate r_U1_U2 with -q1 around the Y axis
A.orient_axis(N, q1, N.y)
q2 = sm.atan2(r_U1_U2.express(A).dot(A.y),r_U1_U2.express(A).dot(A.x))
print('q2 =',q2)

# q3 angle of the upper wishbone reference frame around the axis U1-U2
print('q3 is dependent on q6_initial, this value will be calculated later on.')

# q4 angle between L1 and L2 around the Y-axis (ISO 8855)
q4 = -sm.atan2(r_L1_L2_N.dot(N.z), r_L1_L2_N.dot(N.x))
print('q4 =',q4)

# q5 angle between L1 and L2 around the Z-axis
# First rotate r_L1_L2 with -q4 around the Y axis
B.orient_axis(N, q4, N.y)
q5 = sm.atan2(r_L1_L2.express(B).dot(B.y),r_L1_L2.express(B).dot(B.x))
print('q5 =',q5)

# q6 angle of the lower wishbone reference frame around the axis L1-L2
print('q6 is used as an input value with the initial static value = - 0.139637322383250')

q6_initial = - 0.139637322383250
# Orient local reference frames
```

```
U.orient_body_fixed(N, (q1, q2, q3), 'YZX')              # angles are defined using the right-hand rule
L.orient_body_fixed(N, (q4, q5, q6_initial), 'YZX')      # angles are defined using the right-hand rule

# scalar values for U3_new and L3_new based on initial positions of wire frame and initial angles,
# refer to suspension kinematic model basic to find calculation of these points
U3_pos = (310.004645566198 + U3X_t) * U.x + (433.667215532113 + U3Y_t) * U.y + U3Z_t * U.z
L3_pos = (370.0 + L3X_t) * L.x + (508.176313694371 + L3Y_t) * L.y + L3Z_t * L.z

# New U3 and L3 positions defined in their own reference frames
U3_new.set_pos(U1, U3_pos)
L3_new.set_pos(L1, L3_pos)

#### Plot 3d figure
# Extract coordinates in global frame
points = [U1, U2, U3, L1, L2, L3]
coords = [pt.pos_from(O).express(N).to_matrix(N) for pt in points]

# Convert to numerical values using .item() to extract scalars
coords = [sm.lambdify((), vec, modules='numpy')() for vec in coords]
x_vals = [c[0].item() for c in coords]
y_vals = [c[1].item() for c in coords]
z_vals = [c[2].item() for c in coords]

# Labels
labels = ['U1', 'U2', 'U3', 'L1', 'L2', 'L3']

# Group coordinates into tuples for plotting links
point_dict = dict(zip(labels, zip(x_vals, y_vals, z_vals)))

# Plotting
fig = plt.figure()
ax = fig.add_subplot(111, projection='3d')
ax.scatter(x_vals, y_vals, z_vals, c='r', marker='o')

# Annotate points
for label, (x, y, z) in point_dict.items():
    ax.text(x, y, z, label)

# Plot upper control arm links
for point in ['U1', 'U2']:
    x_line = [point_dict[point][0], point_dict['U3'][0]]
    y_line = [point_dict[point][1], point_dict['U3'][1]]
    z_line = [point_dict[point][2], point_dict['U3'][2]]
    ax.plot(x_line, y_line, z_line, 'b-', label='Upper Control Arm' if point == 'U1' else "")

# Plot lower control arm links
for point in ['L1', 'L2']:
    x_line = [point_dict[point][0], point_dict['L3'][0]]
    y_line = [point_dict[point][1], point_dict['L3'][1]]
    z_line = [point_dict[point][2], point_dict['L3'][2]]
    ax.plot(x_line, y_line, z_line, 'g-', label='Lower Control Arm' if point == 'L1' else "")

# Plot upright link from L3 to U3
x_upright = [point_dict['L3'][0], point_dict['U3'][0]]
y_upright = [point_dict['L3'][1], point_dict['U3'][1]]
z_upright = [point_dict['L3'][2], point_dict['U3'][2]]
ax.plot(x_upright, y_upright, z_upright, 'r--', label='Upright')

# Axis labels and legend
ax.set_xlabel('X [mm]')
ax.set_ylabel('Y [mm]')
ax.set_zlabel('Z [mm]')
ax.set_title('Suspension Hardpoints and Control Arms (ISO 8855)')
ax.legend()
plt.show()

import math
### calculating q3 for a fixed q6 angle
```

```
188
189 # Length of the upright = 329.000655470472, Based on original wireframe positions from
        solidworks, assumed to have zero tolerance.
190 upright = 329.000655470472
191 symbolic = U3_new.pos_from(L3_new).express(N)
192 Constraint = symbolic.magnitude() - upright
193 from sympy import nsolve
194 #print(Constraint)
195
196 # Provide a numerical guess for q3 (in radians), e.g., 0.1
197 q3_numeric = nsolve(Constraint, q3, 0.1)
198 print("q3 (numerical):", q3_numeric)
199
200
201 ### Static camber calculation
202
203 KPI_nominal = -sm.atan2(U3.pos_from(L3).dot(N.y), U3.pos_from(L3).dot(N.z))
204 KPI_nominal_deg = math.degrees(KPI_nominal)
205
206 KPI_tol = -sm.atan2(U3_new.pos_from(L3_new).dot(N.y), U3_new.pos_from(L3_new).dot(N.z))
207
208 temp = KPI_tol.subs(q3, q3_numeric)
209 KPI_tol_deg = math.degrees(temp)
210
211 static_camber = KPI_nominal_deg - KPI_tol_deg
212 print('KPI_nominal:',KPI_nominal_deg)
213 print('KPI_tolerance:', KPI_tol_deg)
214 print('Static camber:', static_camber)
215
216 #### Printing coordinates and lengths
217
218 print('Coordinates in Solidworks coordinate system')
219 print('U1: (S)',U1.pos_from(O).express(S))
220 print('U2: (S)',U2.pos_from(O).express(S))
221 print('U3: (S)',U3_new.pos_from(O).express(S).subs(q3, q3_numeric))
222 print('L1: (S)',L1.pos_from(O).express(S))
223 print('L2: (S)',L2.pos_from(O).express(S))
224 print('L3: (S)',L3_new.pos_from(O).express(S))
225
226 print('Coordinates in ISO 8855 coordinate system')
227 print('U1: (N)',U1.pos_from(O).express(N))
228 print('U2: (N)',U2.pos_from(O).express(N))
229 print('U3: (N)',U3_new.pos_from(O).express(N).subs(q3, q3_numeric))
230 print('L1: (N)',L1.pos_from(O).express(N))
231 print('L2: (N)',L2.pos_from(O).express(N))
232 print('L3: (N)',L3_new.pos_from(O).express(N))
233
234 print('Coordinates in Dynatune coordinate system')
235 print('TI: (D)',TI.pos_from(D).express(N))
236 print('TO: (D)',TO.pos_from(D).express(N))
237 print('L1: (D)',L1.pos_from(D).express(N))
238 print('L3: (D)',L3_new.pos_from(D).express(N))
239 print('L2: (D)',L2.pos_from(D).express(N))
240 print('L3: (D)',L3_new.pos_from(D).express(N))
241 print('U2: (D)',U2.pos_from(D).express(N))
242 print('U3: (D)',U3_new.pos_from(D).express(N).subs(q3, q3_numeric))
243 print('U1: (D)',U1.pos_from(D).express(N))
244 print('U3: (D)',U3_new.pos_from(D).express(N).subs(q3, q3_numeric))
245 print('SU: (D)',SU.pos_from(D).express(N))
246 print('SL: (D)',SL.pos_from(D).express(N))
247 print('WC: (D)',WC.pos_from(D).express(N))
248
249 def format_vector(vec, frame):
250     mat = vec.express(frame).to_matrix(frame)
251     return tuple(round(float(val.evalf()), 4) for val in mat)
252
253 print('Coordinates in Dynatune coordinate system')
254 print('TI: (D)', format_vector(TI.pos_from(D), N))
255 print('TO: (D)', format_vector(TO.pos_from(D), N))
256 print('L1: (D)', format_vector(L1.pos_from(D), N))
257 print('L3: (D)', format_vector(L3_new.pos_from(D), N))
```

```
print('L2: (D)', format_vector(L2.pos_from(D), N))
print('L3: (D)', format_vector(L3_new.pos_from(D), N))
print('U2: (D)', format_vector(U2.pos_from(D), N))
print('U3: (D)', format_vector(U3_new.pos_from(D).express(N).subs(q3, q3_numeric), N))
print('U1: (D)', format_vector(U1.pos_from(D), N))
print('U3: (D)', format_vector(U3_new.pos_from(D).express(N).subs(q3, q3_numeric), N))
print('SU: (D)', format_vector(SU.pos_from(D), N))
print('SL: (D)', format_vector(SL.pos_from(D), N))
print('WC: (D)', format_vector(WC.pos_from(D), N))

print('Do not forget to add static camber value to DynaTune')
print('Static camber:', static_camber)
```

B

Process & Material compatibility and Advanced material search results

Low alloy steels
Low alloy steel, SAE 4130, cast, normalized & tempered (Henricot)
Low alloy steel, SAE 8630, cast, normalized & tempered (Blaw-Knox, Calumetal, Farrel-Cheek, Ohioloy, Quaker)
Low alloy steel, SAE 4130, cast, quenched & tempered (Henricot)
Low alloy steel, SAE 8630, cast, quenched & tempered (Blaw-Knox, Calumetal, Farrel-Cheek, Ohioloy, Quaker)
Low alloy steel, SAE 4335M, cast, quenched & tempered (Superloy)
Cast irons
Cast iron, pearlitic malleable, EN GJMB 600-3, BS EN 1562 (Acipco, Lemax, Lepaz)
Cast iron, pearlitic malleable, EN GJMB 650-2, BS EN 1562 (Acipco, Lemax, Lepaz)
Cast iron, pearlitic malleable, EN GJMB 700-2, BS EN 1562 (Acipco, Lemax, Lepaz)
Cast iron, nodular graphite, EN GJS 700-2, hardened & tempered, BS EN 1563
Stainless steels
Stainless steel, martensitic, ASTM CA-15, cast, tempered at 790°C (Acipco, Afcoloy, Trimrite Stainless)
Stainless steel, martensitic, ASTM CA-15, cast, tempered at 650°C (Acipco, Afcoloy, Trimrite Stainless)
Stainless steel, martensitic, ASTM CA-40, cast, tempered at 650°C (Henricot)
Stainless steel, martensitic, ASTM CA-15, cast, tempered at 595°C (Acipco, Afcoloy, Timrite Stainless)
Stainless steel, martensitic, ASTM CA-40, cast, tempered at 595°C (Henricot)
Stainless steel, martensitic, ASTM CA-15, cast, tempered at 315°C (Acipco, Afcoloy)
Stainless steel, martensitic, ASTM CA-40, cast, tempered at 315°C (Henricot)

Table B.1: Candidate materials considered for suspension lower wishbone redesign resulting from advanced material search from Figure 3.8, materials are listed from left to right corresponding to Figure 3.9.

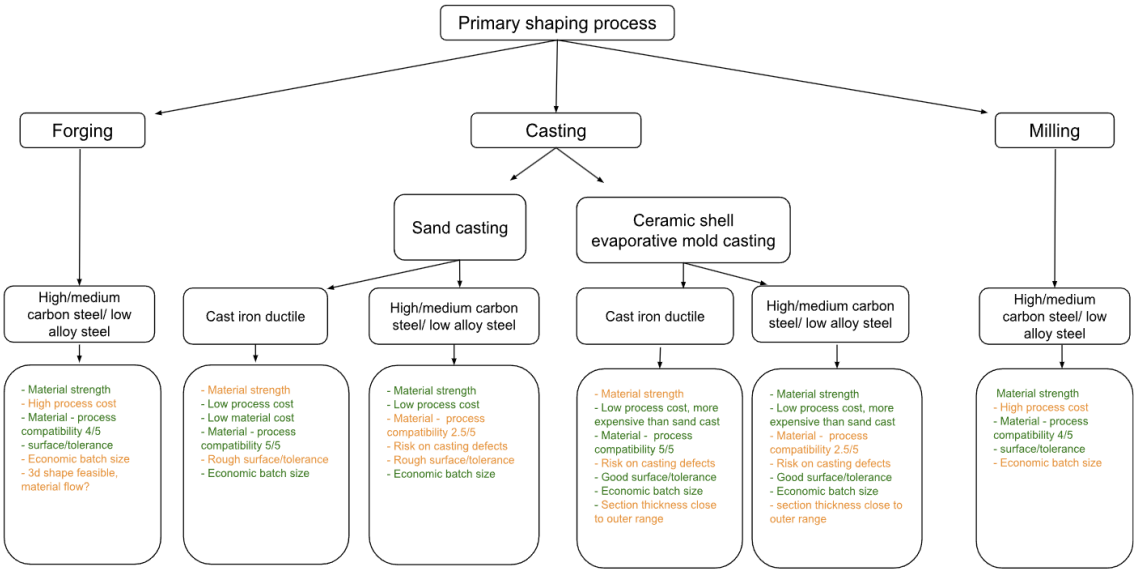

Figure B.1: Process and material compatibility and advantages/disadvantages of process/material combinations.

C

Requirement matrix & market analysis

Requirement	Double wishbone	Solid Axle	De Dion
R1	Proven compatibility (GRF, Mammoth)	Unknown, no examples of compatibility	Unknown, no examples of compatibility
R2	Feasible	Feasible, no examples of compatibility with R2 and R3.	Feasible
R3	Feasible	Feasible, no examples of compatibility with R3 and R2.	Feasible (Mowag Eagle V)
R4	• Ground clearance feasible, dependent on payload • Breakover angle feasible • Approach/departure angle feasible • Static tilt angle unsure, lower COG height compared to solid axle and De Dion	• Ground clearance feasible, independent on payload • Breakover angle feasible • Approach/departure angle feasible • Static tilt angle unsure, higher overall COG height compared to double wishbone	• Ground clearance feasible, independent on payload • Breakover angle feasible • Approach/departure angle feasible • Static tilt angle unsure, higher overall COG height compared to double wishbone
R5	Feasible	Feasible	Feasible
R6	Feasible	Feasible	Feasible

Table C.1: Compatibility of suspension architectures with system requirements. The assessment is based on documented examples of existing vehicles as well as feasibility assumptions where direct examples are not found.

Table C.2: Market analysis of military terrain vehicles.

Vehicle	Architecture	Clearance [mm]	Protection	GVW [kg]	Dimensions [m]
Supacat HMT Extenda MK3	Double wishbone, adjustable height	180–485	Mine blast and ballistic	9000	5,8 × 2,1 × 1,9
Iveco Manticore	Solid axle	350	Mine blast and ballistic	12500	5,9 × 2,4 × 2,8
Iveco DMV Anaconda 9	Independent front, solid axle rear	500	Optional ballistic	6000	5,3 × 2,2 × 2,3
Defenture GRF	Double wishbone	340	Modular ballistic	4600	5,1 × 1,8 × 2,2
Defenture Mammoth	Double wishbone	366	Mine blast and ballistic	8800	5,7 × 2,1 × 2,3
ACS ENOK 7.5	Solid axle + portals	420	Mine blast and ballistic	7500	4,8 × 2,2 × 2,2
Humvee NXT 360	Double wishbone	437	Mine blast and ballistic	7100	5,1 × 2,2 × 2,1
GDE MOWAG EAGLE 5	De Dion	400	Mine blast and ballistic level 2	10000	5,4 × 2,2 × 2,3
Soframe VENPIR	Double wishbone	550	Mine level 1, ballistic optional	11500	6,2 × 2,5 × 2,5
Oshkosh JLTV	Double wishbone	411	Optional level 3	10200	6,2 × 2,5 × 2,6
Nimr AJBAN MK2	Double wishbone	505	Mine blast level 3 and ballistic level 4	11500	5,6 × 2,4 × 2,3
INKAS APC – Titan LLC	Solid axle	–	Mine blast and ballistic level 2	9080	6,0 × 2,3 × 3,3
Streit Spartan SUT–MAV	Solid axle	450	Mine blast and ballistic level 2	8800	6,3 × 2,5 × 2,4
Lenco BearCat G3	Solid axle	355	Mine blast and ballistic	11000	6,3 × 2,5 × 2,4
Streit Scorpion	Double wishbone	–	Mine level 2+, Ballistic level 3, level 4 optional	11000	6,8 × 2,5 × 2,4
MOWAG Duro	De Dion	–	–	11000	6,0 × 2,0 × 2,7
Arquus Sherpa Light Scout	Solid axle	330	Mine blast and ballistic	6850	5,4 × 2,9 × 2,1
Fering Pioneer X	Independent, adjustable height	800	Mine blast and ballistic	1650	5,1 × 1,9 × 1,7
General Dynamics Foxhound	Double wishbone	350	Mine blast and ballistic	8500	5,4 × 2,1 × 2,3

D

SimSolid structural analysis results

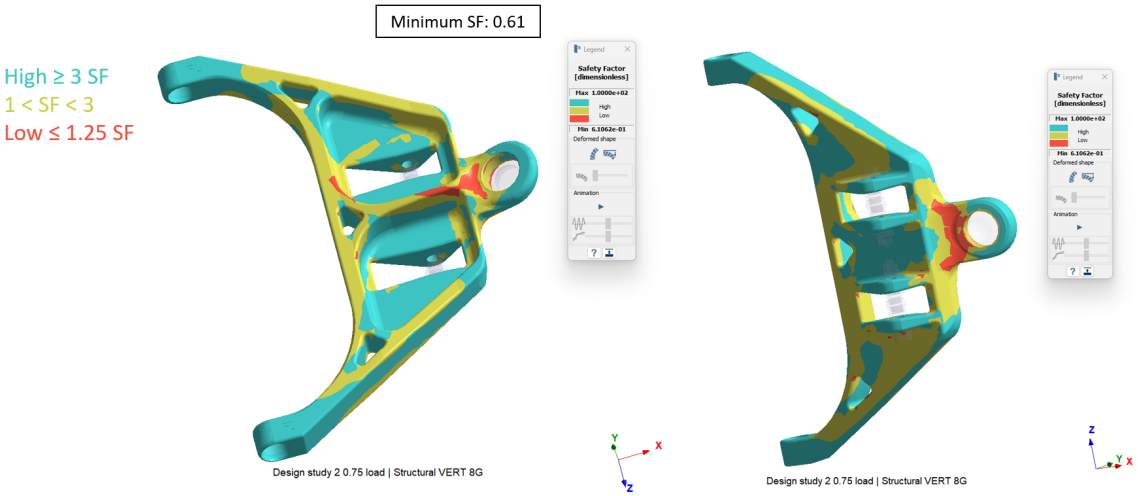

Figure D.1: Structural analysis of the lower wishbone redesign using pearlitic malleable, EN GJMB 600-3 cast iron steel and the extreme drop test load case.

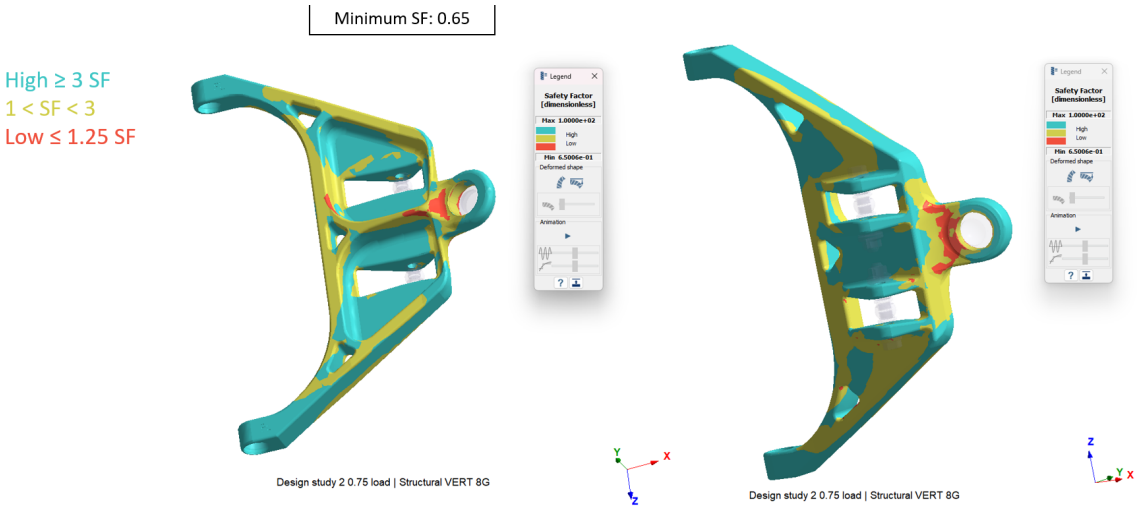

Figure D.2: Structural analysis of the lower wishbone redesign using pearlitic malleable, EN GJMB 650-2 cast iron steel and the extreme drop test load case.

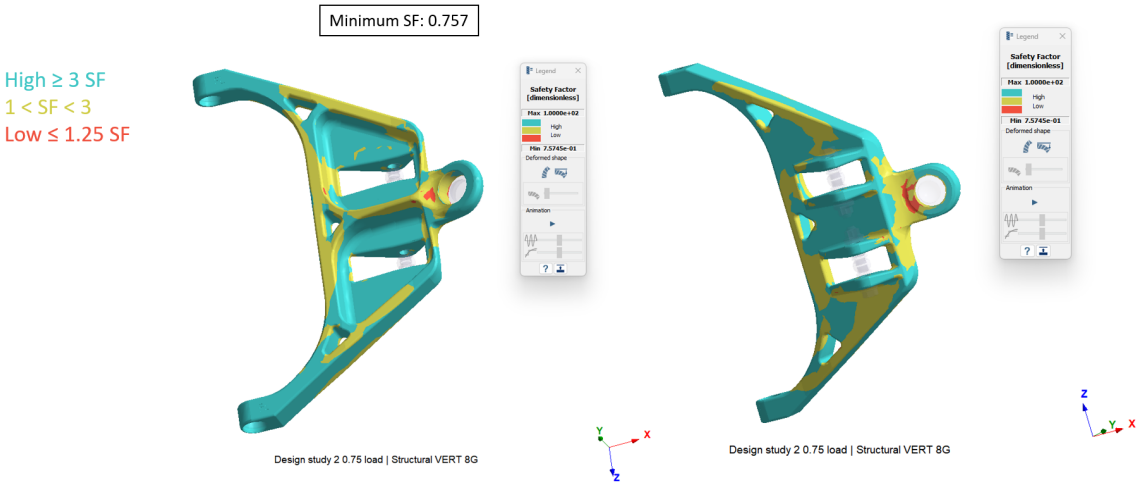

Figure D.3: Structural analysis of the lower wishbone redesign using pearlitic malleable, EN GJMB 700-2 cast iron steel and the extreme drop test load case.

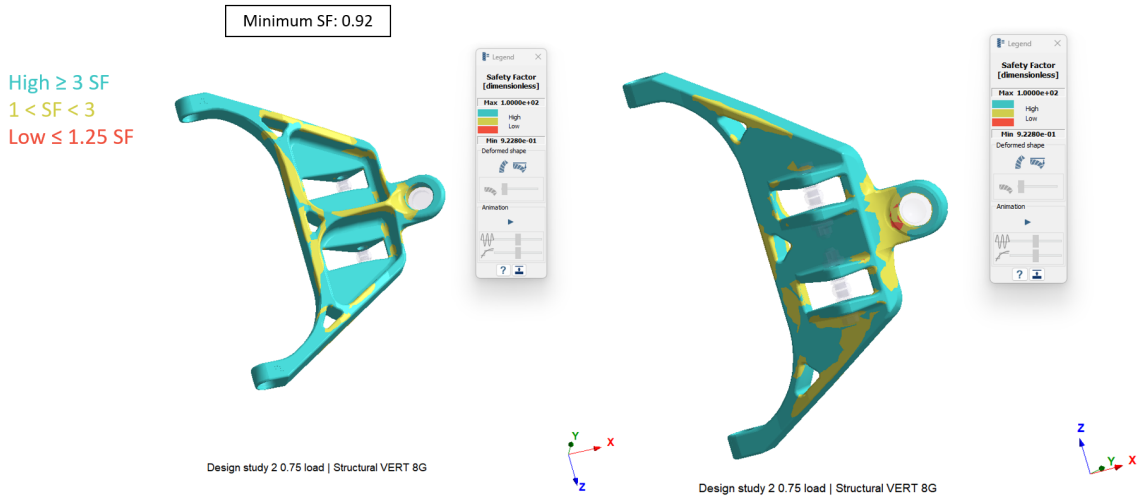

Figure D.4: Structural analysis of the lower wishbone redesign using SAE 4130 low alloy steel and the extreme drop test load case.

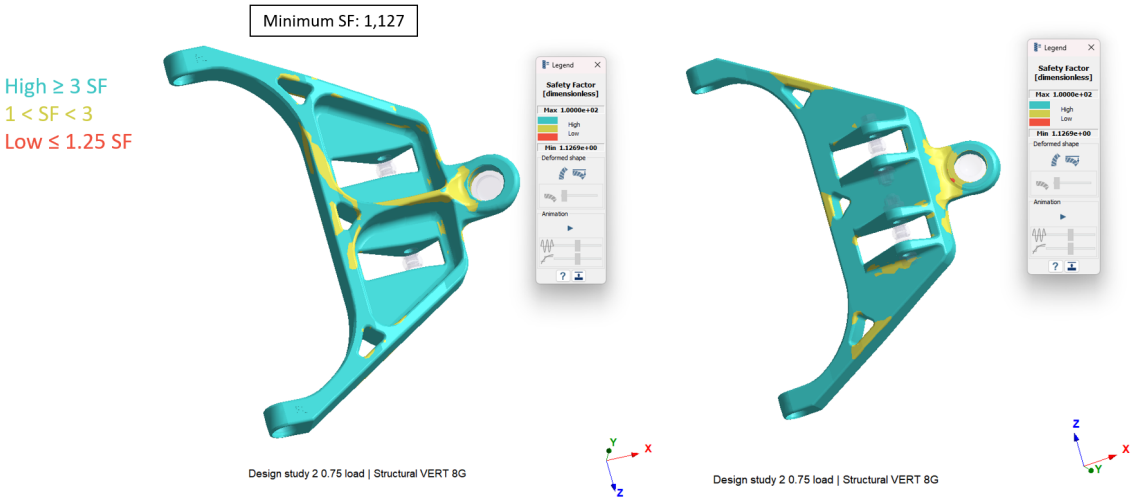

Figure D.5: Structural analysis of the lower wishbone redesign using SAE 8630 low alloy steel and the extreme drop test load case.

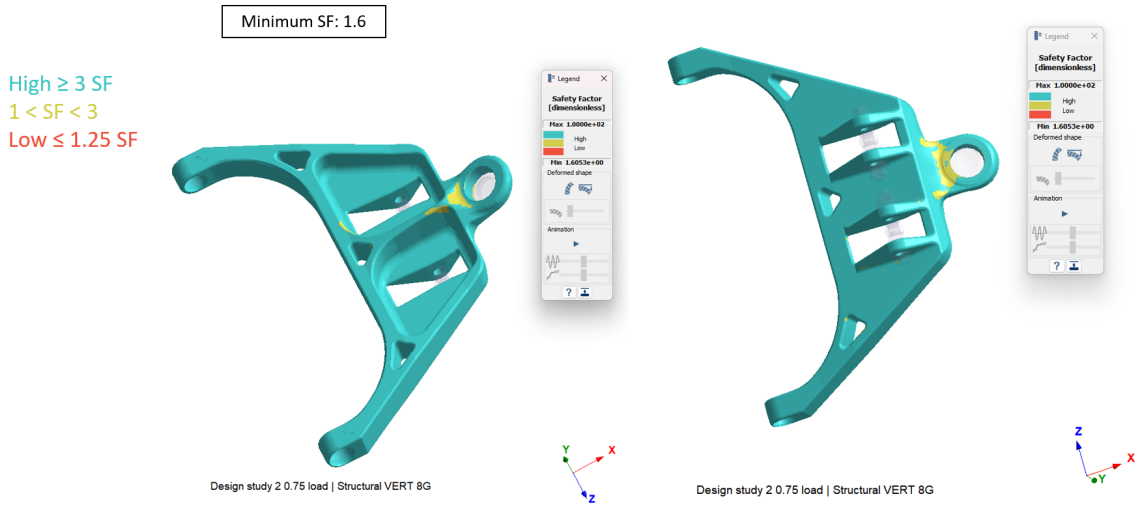

Figure D.6: Structural analysis of the lower wishbone redesign using SAE 4335M low alloy steel and the extreme drop test load case.

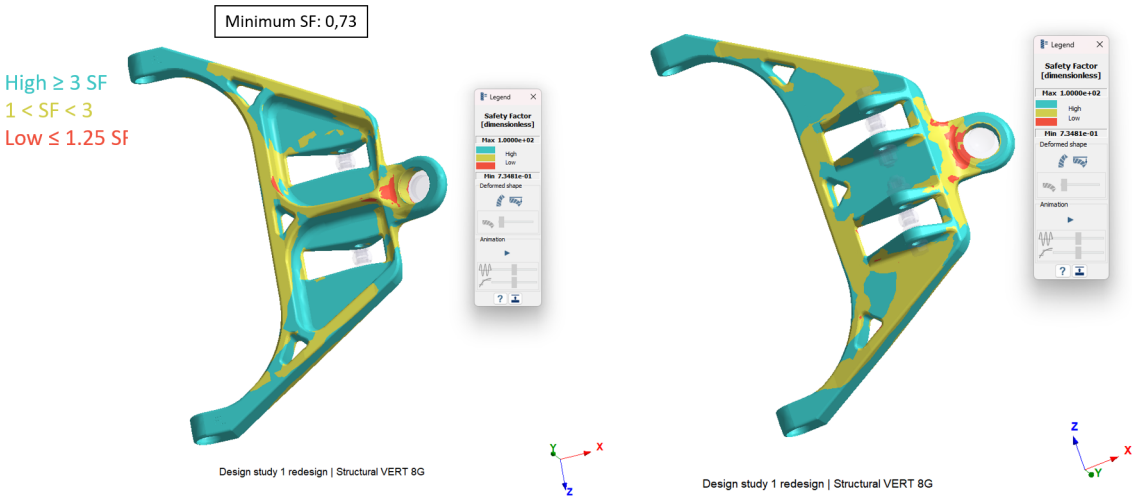

Figure D.7: Structural analysis of the lower wishbone redesign using SAE 4130 low alloy steel and the extreme drop test load case of the rear axle.

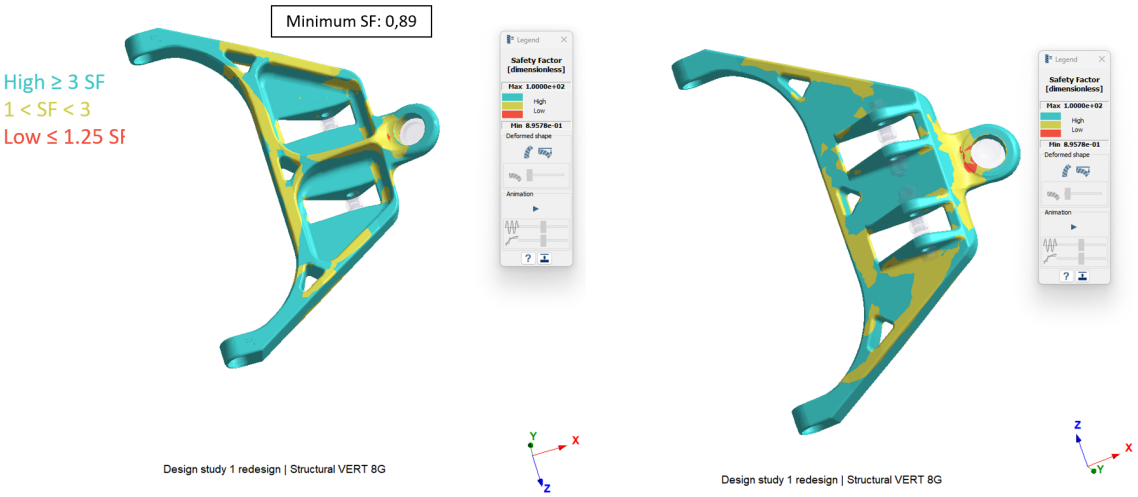

Figure D.8: Structural analysis of the lower wishbone redesign using SAE 8630 low alloy steel and the extreme drop test load case of the rear axle.

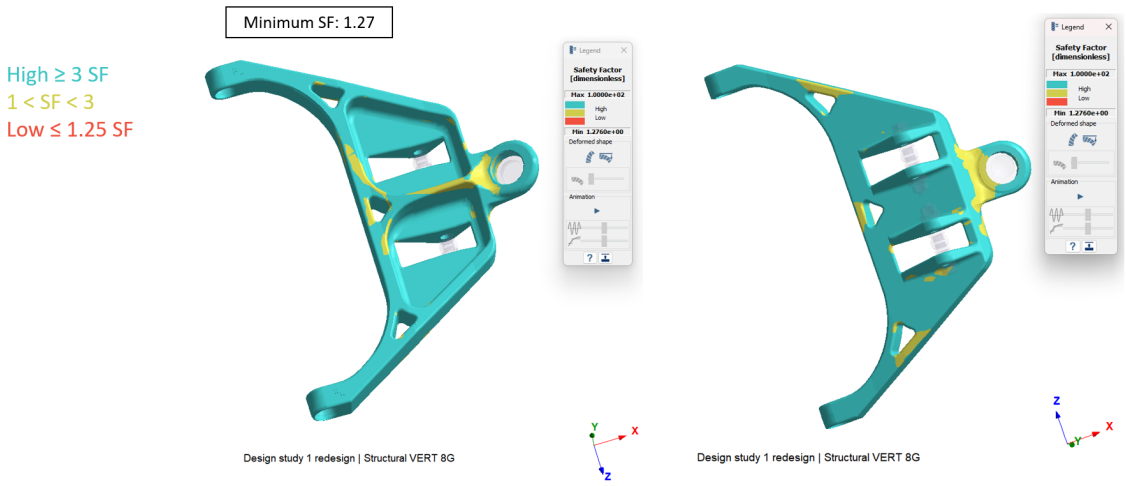

Figure D.9: Structural analysis of the lower wishbone redesign using SAE 4335M low alloy steel and the extreme drop test load case of the rear axle.

		Front axle load			Rear axle load		
Material	**Low alloy steel**	**SAE 4130**	**SAE 8630**	**SAE 4335M**	**SAE 4130**	**SAE 8630**	**SAE 4335M**
		Safety factor			Safety factor		
Maximum	Vertical 7G	1,01	1,23	1,76	0,83	1,01	1,44
	Longitudinal FWD 4G	1,51	1,85	2,63	1,15	1,4	1,99
	Longitudinal RWD 4G	1,26	1,53	2,18	1,02	1,24	1,76
	Lateral IW 3G	1,78	2,17	3,1	1,38	1,68	2,39
	Lateral OW 3G	1,74	2,13	3,03	1,68	2,05	2,91
Extreme	Vertical 8G	0,92	1.13	1.61	0,73	0,9	1,28
	Longitudinal FWD 5G	1,23	1,5	2,13	0,92	1,12	1,6
	Longitudinal RWD 5G	1,09	1,33	1,89	0,82	1	1,42

Figure D.10: Minimum safety factors for all load cases across the low alloy steels, rear load case included as reference.

E

Steering system tolerance analysis

During the project, an additional tolerance analysis was conducted to evaluate the effect of tolerances in the steering system on the toe angle of the front wheels during wheel travel.

Tolerance chains were defined from the chassis to the inner ball joint of the toe link in both the Y and Z direction, following the coordinate systems defined in ISO 8855. Tolerances in the X direction were assumed to have a negligible impact on the toe angle and were therefore initially excluded from the analysis.

The steering hardpoint locations, along with their tolerances, were used as input to plot the toe angle against wheel travel using the DynaTune Suspension Design Module.

To simplify the analysis, the following assumptions were made:

- Ball joints are considered ideal, with zero play and no positional.
- All components are modeled as rigid bodies, with no compliance or deformation.
- Steering gear tolerances are assumed to be zero due to the absence of tolerance data.
- In all scenarios, the toe link length is adjusted to achieve the desired static toe angle.

The tolerance chains in the Y and Z direction are shown in Figures E.1 and E.2. The toe angle variations during wheel travel are shown in Figures E.4 and E.5. To validate the assumption regarding the X direction, a variation of $\pm$ 2 mm was introduced to analyze the effect on the toe angle (Figure E.3). The results confirm that tolerances in the X direction have a negligible effect compared to those in the Y and Z directions.

A key observation is that tolerances in the Z direction have the most significant impact on the toe angle variation. Additionally, the largest deviation from the nominal toe angle occurs at full bump of the suspension, this can be attributed to the longer upward stroke of the suspension compared to the downward stroke.

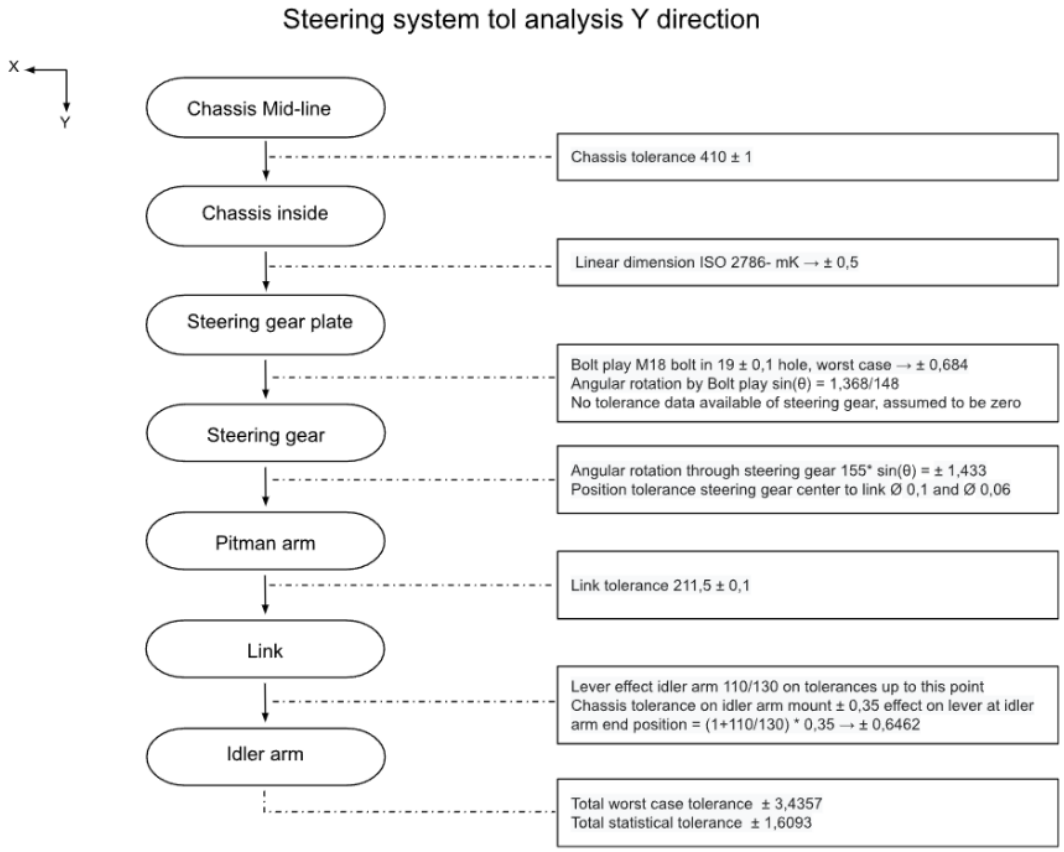

Figure E.1: Tolerance chain of the steering system in the Y direction, using statistical and worst case tolerances.

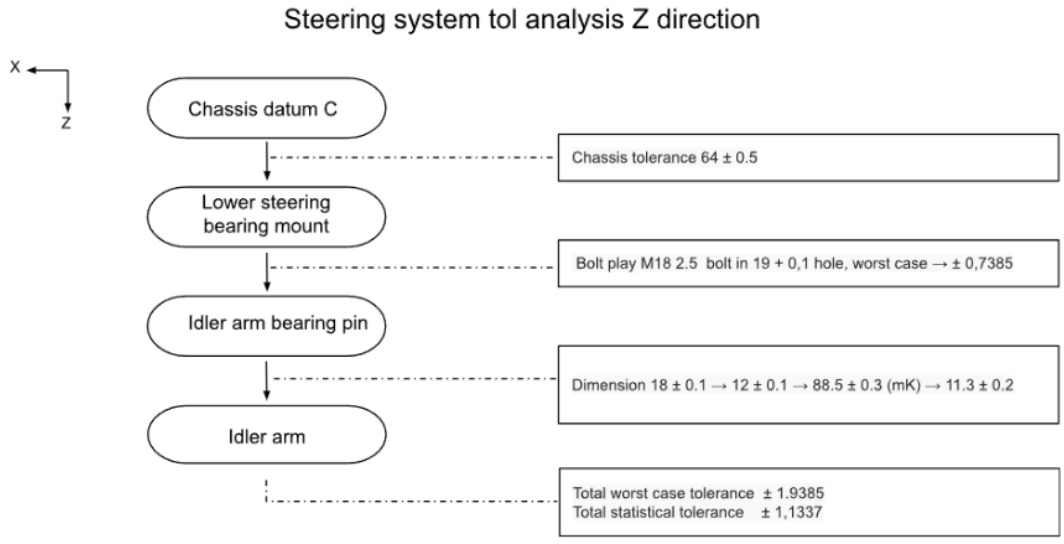

Figure E.2: Tolerance chain of the steering system in the Z direction, using statistical and worst case tolerances.

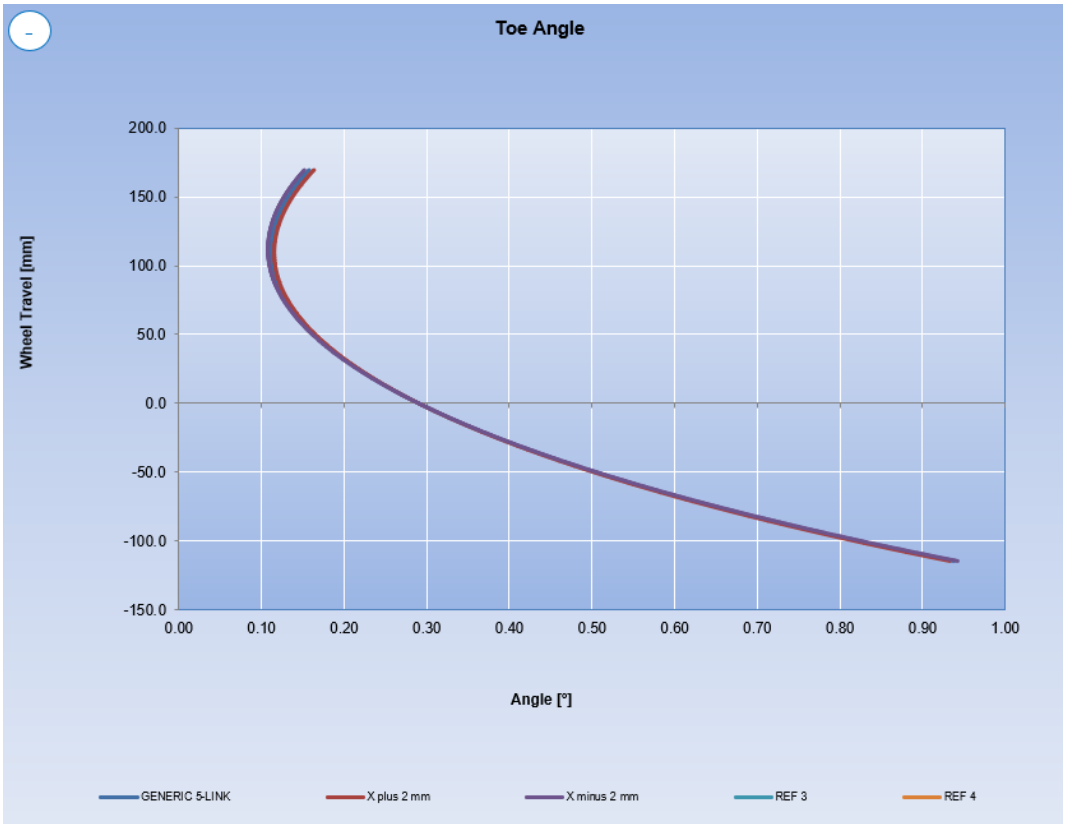

Figure E.3: Toe angle effect by $\pm$ 2 mm variation in the X direction.

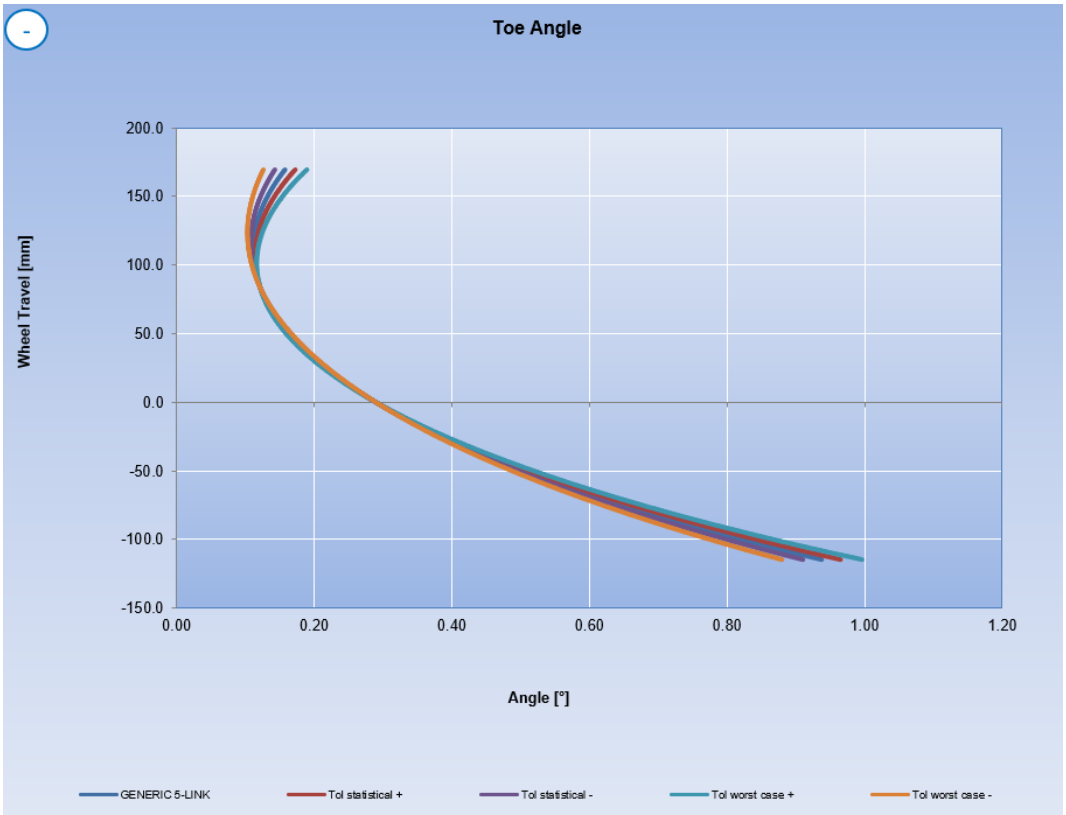

Figure E.4: Toe angle impacted by steering system tolerances in the Y direction.

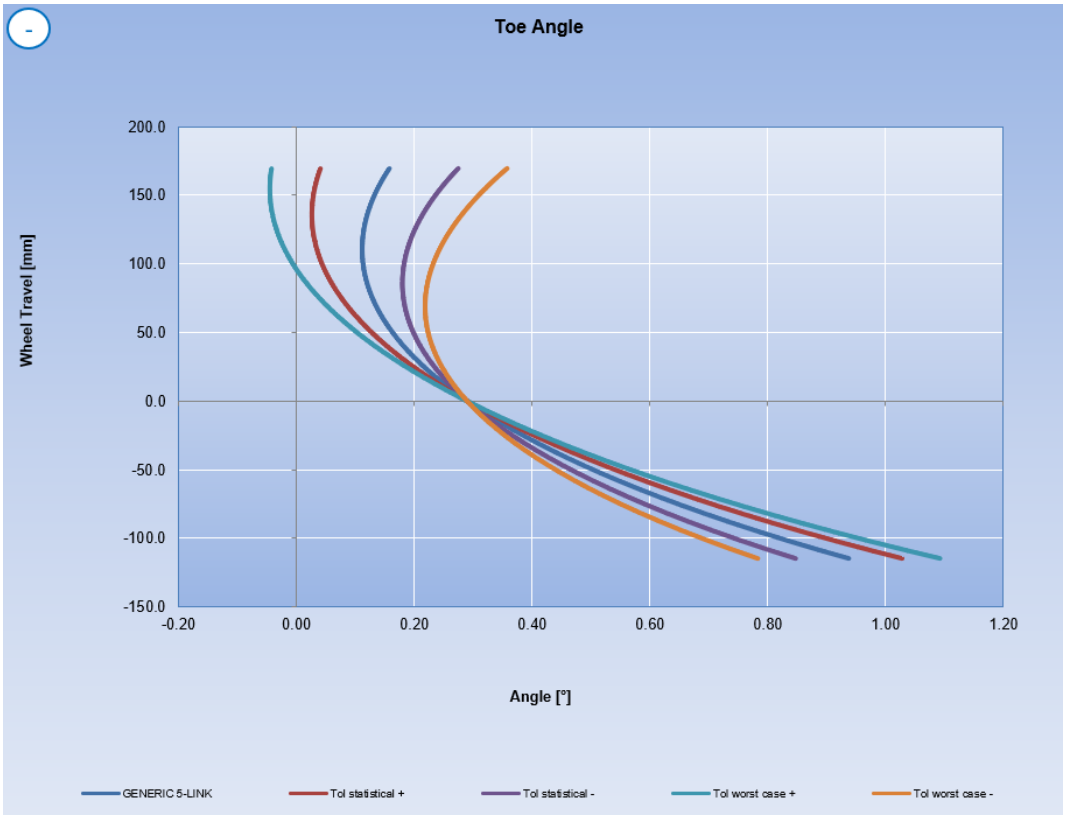

Figure E.5: Toe angle impacted by steering system tolerances in the Z direction.

F

Original design of the lower wishbone

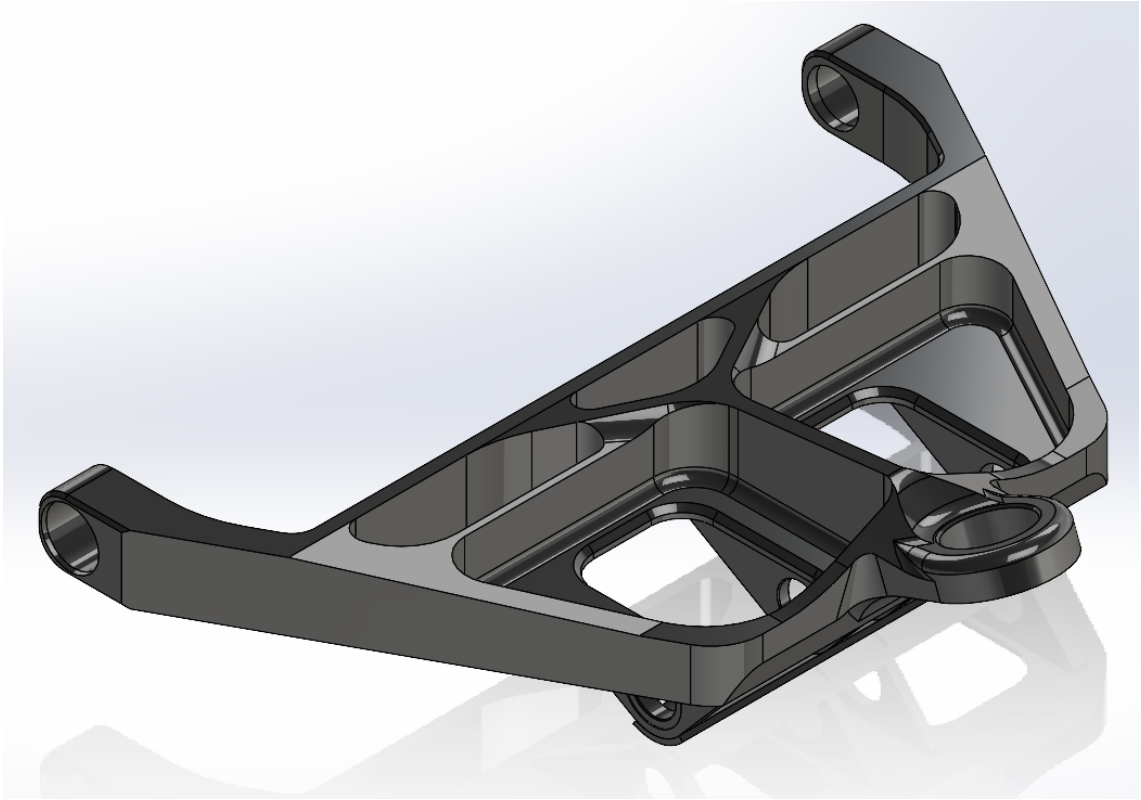

Figure F.1: CAD model of the prototype lower wishbone in SolidWorks.

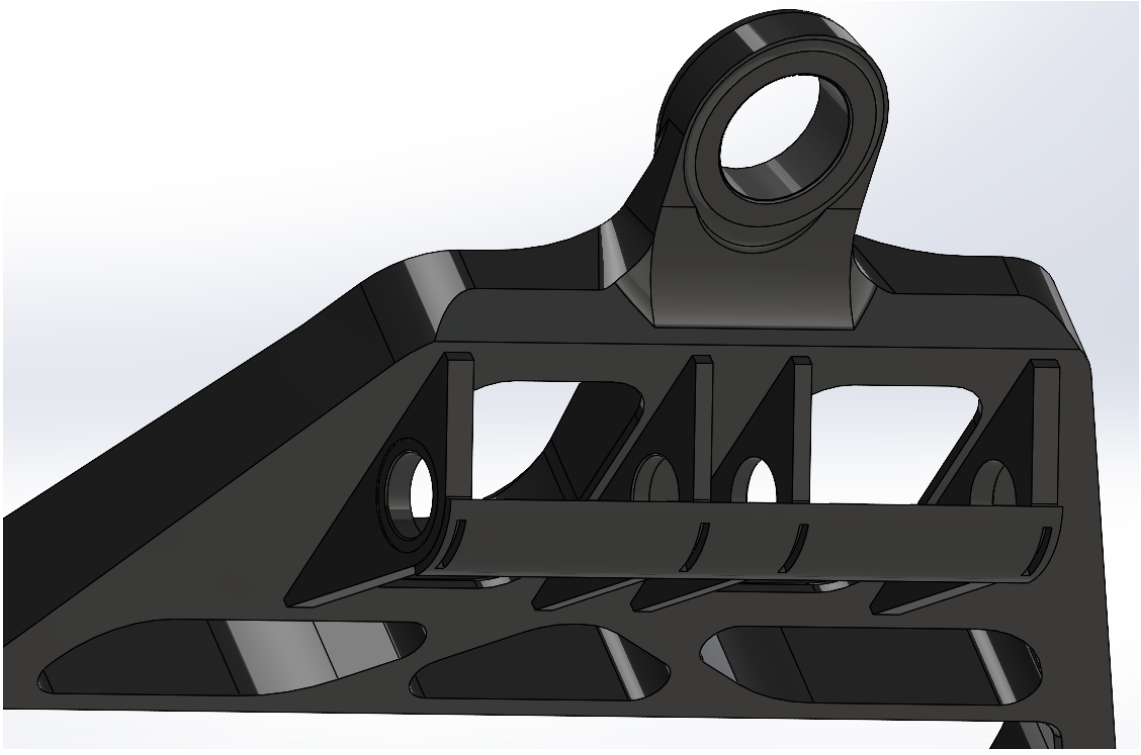

Figure F.2: CAD model of the prototype lower wishbone in SolidWorks, zoomed in on the interfaces for the shock absorbers and the outer ball joint interface.